

Universidade de Lisboa

Faculdade de Farmácia

University of Helsinki

Faculty of Pharmacy



## **Characterization of Olanzapine and Polymer Orodispersible films**

Ana Maria Gaspar Ventim Neves

Mestrado Integrado em Ciências Farmacêuticas

2017

Universidade de Lisboa

Faculdade de Farmácia

University of Helsinki

Faculty of Pharmacy



## **Characterization of Olanzapine and Polymer Orodispersible films**

Ana Maria Gaspar Ventim Neves

Monografia de Mestrado Integrado em Ciências Farmacêuticas apresentada à Universidade de Lisboa através da Faculdade de Farmácia

Supervisors:

Prof. Clare Strachan, Pharmaceutical Technology and Chemistry, Faculty of Pharmacy of the University of Helsinki

Prof. João Pinto, Departamento Tecnologia Farmacêutica, Faculdade de Farmácia da Universidade de Lisboa

2017

## Abstract

The use of orodispersible films has gained increasing relevance among solid pharmaceutical forms. They consist of a thin and flexible polymeric film, formulated to rapidly disintegrate in the oral cavity. Being a solid dispersion, the solid characterization of its components is of utmost importance, as it dictates the physical stability and safety of the product. The aim of this work was to characterize the drug-polymer compatibility and the solid state of a poorly water-soluble drug (olanzapine) in a polymeric orodispersible matrix, as a primary stage of product development. Methocel<sup>®</sup> (HPMC) and Soluplus<sup>®</sup> were chosen as matrix-former polymers, based on their wide-usage in previous works. Olanzapine orodispersible films were obtained through solvent-casting technique, using methanol as solvent and a proportion of drug-polymer of 1:1 (m/m %). Spectroscopic studies (Raman, FTIR, CARS, TimeGated<sup>®</sup> Raman) and thermodynamic studies (DSC) were performed to characterize olanzapine's solid state within the orodispersible matrix. Polarized light microscopy showed refringence, thus, revealing the presence of crystals in the both Olz-HPMC and Olz-Soluplus films. Comparing to the assignment made in previous works and to the spectra obtained in this work, spectroscopic data showed peaks that did not correlate neither to form 1 nor to form 2. Furthermore, peaks were found to be shifted towards higher wavenumbers, namely peaks assigned to NH deformations. This suggests that an interaction between the drug and the polymer could be occurring. DSC data supports this hypothesis, as olanzapine's melting point in both drug-polymer films and physical-mixtures revealed a  $T_{\text{onset}}$  severely lower than form 1 melting point. This work suggests that there appears to be an interaction between drug and polymers, which is proposed to be occurring through H bonding. Nonetheless, this interaction could be favourable as it could be interesting to stabilize small dimension crystals or even amorphous form of olanzapine.

## Keywords

Orodispersable films, Olanzapine, Polymorphism, Interaction

## Resumo

Os filmes orodispersíveis constituem uma forma farmacêutica que tem ganho algum destaque no âmbito das formas farmacêuticas sólidas. Representam filmes poliméricos, delgados, flexíveis, formulados com o intuito de se desintegrarem rapidamente na cavidade oral, sem recurso a líquidos que auxiliem a deglutição. Ao se tratarem de dispersões sólidas, torna-se imprescindível a caracterização do estado sólido dos seus compostos, bem como o estudo de possíveis interações entre os diferentes componentes, tendo em vista a estabilidade física e segurança do produto final. Uma substância pode ser encontrada sob diferentes formas polimórficas, formas solvatadas ou ainda no estado amorfo, sendo que cada forma possui diferentes propriedades físico-químicas. Em última instância, toda esta variabilidade tem repercussões na biodisponibilidade da própria substância ativa. Durante a otimização de uma forma farmacêutica sólida, o balanço entre estabilidade e solubilidade tem que ser obtido, uma vez que estes dois fatores nem sempre se mostram compatíveis. Por exemplo, o estado amorfo apresenta taxas de dissolução mais elevadas, por não ser necessário ultrapassar as energias de coesão que um cristal possui. Ainda assim, este estado sólido apresenta a desvantagem de ser mais instável, ocorrendo cristalização durante o tempo de prateleira do produto. Uma estratégia interessante para estabilizar e alterar a taxa de dissolução de SA passa pela sua incorporação numa matriz solúvel em água, i.e, pela formulação de uma dispersão sólida. Para tal, recorre-se a polímeros capazes de formar uma matriz que, pela sua incapacidade de possuir um arranjo cristalino de grandes dimensões, criam uma estrutura na qual as moléculas (ou pequenos cristais) do fármaco se intercalam. Neste projeto, filmes orodispersíveis de olanzapina e dos polímeros HPMC e Soluplus<sup>®</sup> foram produzidos pela técnica de espalhamento (utilizando-se metanol como solvente), visando o estudo da compatibilidade entre a substância ativa e cada polímero, bem como a caracterização do estado sólido da olanzapina nos filmes obtidos. Para tal, recorreu-se a técnicas espectrofotométricas (Raman, FTIR, TimeGated<sup>®</sup> Raman e CARS) e, ainda, a estudos termodinâmicos (DSC). No âmbito do estudo de compatibilidade, proporções 1:1 (olz-polímero) foram utilizadas tanto nas misturas físicas como nos próprios filmes desenvolvidos, por se tratar da proporção que favorece a interação máxima entre os compostos. Os resultados revelaram que a matéria-prima de olanzapina se constituía pela forma polimórfica conhecida na literatura como forma 1 (polimorfo mais estável) e as suas características foram tidas como referência nos estudos efetuados posteriormente. No caso das misturas físicas, as principais características desta forma mantiveram-se preservadas, sem grandes alterações nos perfis analíticos. Ainda assim, a análise espectrofotométrica revelou ligeiras alterações que sugerem que alguma interação entre olz-polímero possa ocorrer. Mais precisamente, as bandas correspondentes a grupos moleculares envolvidos em ligações de hidrogénio encontraram-se com desvios, tendo-se observado este facto tanto no caso do polímero HPMC como para o Soluplus. Adicionalmente, o perfil do DSC revelou um ponto de fusão desviado relativamente ao obtido para a matéria-prima de olanzapina. Estes dois resultados sugerem que alguma interação possa ocorrer entre o fármaco e cada um dos polímeros. Quanto aos filmes olz-polímero, as alterações observadas são ainda mais acentuadas e complexas de se analisar. Os picos espectrofotométricos tidos como referência para a forma 1 de olanzapina revelaram alterações importantes. Sendo que a interpretação pode passar pela presença de olanzapina no estado amorfo, bem como a da presença de metanolato no filme final. Não foram encontrados dados espectrofotométricos relativos a estas formas sólidas na literatura, pelo que um próximo passo seria a sua caracterização detalhada com o intuito de se comparar com os espectros dos filmes obtidos.

**Palavras-Chave:** Filmes Orodispersíveis, Olanzapina, Polimorfismo, Interação

# Table of Contents

1. Introduction .....	7
1.1 Solid State .....	7
1.2 Solid State Characterization .....	9
1.3 Solid Form of Olanzapine .....	14
1.4 Polymers .....	18
1.5 Gap in the literature .....	20
2. Aim .....	20
3. Materials and Methods .....	20
3.1 Solubility Analysis .....	20
3.2 Preparation of the samples .....	20
3.3 Polarized Light Microscopy .....	21
3.4 Spectrophotometry .....	21
3.5 DSC .....	21
3.6 Data Analysis .....	21
4. Results .....	22
4.1 Solubility Analysis .....	22
4.2 Observational characterization of fresh made film .....	22
4.3 Polarized Light Microscopy .....	23
4.4 Spectroscopic Characterization .....	25
4.5 DSC characterization .....	34
5. Discussion .....	38
5.1 Starting Materials - Powders .....	38
5.2 Physical Mixtures and Final Products .....	38
6. Conclusion .....	41
7. Further Studies .....	42
8. References .....	43

## List of Figures

Fig. 1 Diagram of Raman scattering phenomenon, alongside resonance and fluorescence effect.....	11
Fig. 2 Diagram of the radiation frequencies and vibrational transitions involved in CARS process.....	12
Fig. 3 Molecular structure of olanzapine.....	14
Fig. 4 a) Molecular diagram of the crystal building block, from reference (23); b) Crystal building block, from reference (25).....	16
Fig. 5 Molecular structure of HPMC.....	19
Fig. 6 Molecular structure of Soluplus.....	19
Fig. 7 Obtained films containing: a) HPMC film (100% polymer); b) Soluplus film (100% polymer); c) HPMC-Olz film (50% m/m Polymer-Drug); d) HPMC-Olz film (50% m/m Polymer-Drug); e) Soluplus-Olz film (50% m/m Polymer-Drug); f) Soluplus-Olz film (50% m/m Polymer-Drug).....	23
Fig. 8 a) HPMC-Olz Film; Amp. 10x; b) HPMC-Olz Film; Amp. 10x; c) HPMC-Olz Film; Amp. 40x; d) HPMC-Olz Film; Amp. 40x; e) Soluplus-Olz Film; Amp. 10x; f) Soluplus-Olz Film; Amp. 10x; g) Soluplus-Olz Film; Amp. 40x; h) Soluplus-Olz Film; Amp. 40x.....	24
Fig. 9 Raman spectrum of Olz, HPMC and Soluplus Powder: a) full spectra; b) Raman shift 1400-1700 $\text{cm}^{-1}$ .....	25
Fig. 10 ATR IR spectrum of Olz, HPMC and Soluplus powders: a) full spectra; b) 1400-1700 $\text{cm}^{-1}$ and c) 2600-3600 $\text{cm}^{-1}$ .....	26
Fig. 11 Raman spectrum of HPMC-Olz physical mixture and film: a) full spectra; b) Raman shift 1400-1700 $\text{cm}^{-1}$ .....	28
Fig. 12 ATR IR spectrum of HPMC-Olz physical mixture and film: a) full spectra; b) 1400-1700 $\text{cm}^{-1}$ and c) 2600-3600 $\text{cm}^{-1}$ .....	29
Fig. 13 Raman spectrum of Soluplus-Olz physical mixture and film: a) background; b) Raman shift 1400-1700 $\text{cm}^{-1}$ .....	30
Fig. 14 ATR IR spectrum of Soluplus-Olz physical mixture and film: a) full spectra; b) 1400-1700 $\text{cm}^{-1}$ and c) 2600-3600 $\text{cm}^{-1}$ .....	31
Fig. 15 TGR spectrum of Olanzapine powder, Soluplus film and HPMC film in a range 264-3100 $\text{cm}^{-1}$ .....	32
Fig. 16 CARS imaging of: a) olanzapine powder - $\omega_n = 1517 \text{ cm}^{-1}$ ; b) HPMC-Olz film - $\omega_n = 1517 \text{ cm}^{-1}$ ; c) Soluplus-Olz film - $\omega_n = 1517 \text{ cm}^{-1}$ .....	33
Fig. 17 DSC curve of olanzapine powder.....	34
Fig. 18 DSC curve of HPMC and Soluplus powder.....	35
Fig. 19 DSC curve of: a) HPMC-Olz physical mixture and HPMC-Olz film; b) Soluplus- Olz physical mixture and Sol-Olz film.....	36

## List of tables

Table 1 Methods used in solid state characterization. ....	9
Table 2 Summary of the enthalpic transitions detected by DSC (18). ....	13
Table 3 List of peaks of interest, produced according to Ayala's work (23) and the obtained spectrum.....	27
Table 4 Compilation of DSC data obtained from olanzapine raw material, HPMC-Olz and Soluplus-Olz both physical mixture and film.....	37

## List of abbreviations

BCS – Biopharmaceutical classification system
CARS – coherent anti-Stokes Raman spectroscopy
CSD – crystallographic structure database
DSC – differential scanning calorimetry
FTIR- ATR – Fourier-transform infrared – attenuated total reflectance
HPMC – hydroxypropyl methylcellulose
MDSC - modulated differential scanning calorimetry
MIR – mid-Infrared
NIR – near-infrared
Olz – olanzapine
PLM - polarized light microscopy
SEM – scanning electron microscopy
Sol – Soluplus
Tg – glass transition emperature
UV – ultra-violet
Wn – wavenumber

# 1. Introduction

With the development of pharmaceutical technology new techniques have arisen and others have improved to overcome obstacles that once seemed impossible to resolve. With the aim of answering some of the unresolved medical conditions that pharmaceutical industry still faces, new production challenges keep arising. In this sense, an overwhelming amount of methods and applications have been gaining more attention, not only in the field of product development but also in its characterization.

Solid forms are still the majority of pharmaceutical products found in the market, and represent one of the fields where innovation is most seen. Nevertheless, there is still room for improvement. One very interesting application is drug-loaded orodispersible films, which are known by their ability to deliver a stabilised active ingredient through a rapid disintegration in the oral cavity (1).

The aim of this work was to characterize the drug-polymer compatibility and the solid state of a poorly water-soluble drug (olanzapine) in a polymeric orodispersible matrix, as a primary stage of product development.

## 1.1 Solid State

It is well known that the solid state of a substance dictates its physical-chemical behaviour, and can ultimately affect the production process and the final performance of the product. The solid-state characteristics such as morphology, particle size, polymorphism, solvation and hydration affect a variety of properties as filtration, flow, dissolution and, consequently, bioavailability and therapeutic effect (2, 3). Ultimately, the crystal habit determines the formulation processes and the pharmaceutical form of the final product. Hence, even though different crystal polymorphs may have similar absorption rates, the bioavailability of the final product may differ based on how the drug can be formulated (2).

Although much progress has been made in the field, it is not yet possible to predict neither the crystal structures nor their physical properties based on the molecular structure of a drug (2, 3). One very interesting example of the progress made in the field is the work developed by Bhardwaj *et al.* (4) where an experimental vs computed crystal energy landscape of olanzapine was explored. The authors found that, even though the extensive energy landscape screening has clarified some of the findings of previous works, probably, it has not found all possible physical forms of olanzapine. Therefore, the assessment and control of the drug's solid form during production is of utmost importance to obtain safe and efficient medicines that satisfy the regulatory requirements and respect intellectual property of other products that are already being commercialized (3). For instance, to the best of our knowledge, there is more than twenty patents claiming different crystal forms of olanzapine as well as different preparation processes. Thus, the molecule of the active ingredient may not be patentable, but instead, its crystal form, solvates or amorphous forms can be intellectually protected.

In this matter, the present work will study in detail the solid form of olanzapine in an orodispersible matrix.

### 1.1.1 Polymorphs

When the molecules of a substance organize in different ways within the crystal lattice, it's called a polymorph. As a result of the different possible arrangements, there can be different crystal forms of a same compound (2, 3). The differences in the molecular packing, orientation and conformation of each polymorph confer different Gibbs free energy to each crystal form.



Thus, each one has a specific melting point, stability, solubility and overall pharmaceutical behaviour (2, 3).

The most stable polymorph is the one with the lowest Gibbs free energy, which is to say the most thermodynamically favourable, and the tendency is that all the other polymorphs tend to transform into it under the same conditions (2). From a production perspective, the most stable polymorph is the preferable one, which would result in thermodynamic stability in the final product. However, there are multiple factors that can influence the crystallization, and thus a considerable amount of time and effort have to be made to determine the specific conditions that lead to the desired form (3).

### **1.1.2 Solvates**

When molecules of the solvent are incorporated into the structure of the crystal, becoming part of the crystal lattice, the resulting product is called a solvate. When that solvent is water it is called a crystal hydrate (2, 3). Not so often, it is possible to find the term “pseudo-polymorph” when referring to solvates.

This integration of the solvent within the crystal structure is a consequence of the interactions between the solvent and the drug molecules, which can be of many natures. Some solvents have a vital importance within the structure in holding the solvate crystal together. For instance, their molecules can interact via hydrogen bonding with the drug, thus making a very stable net that is difficult to disrupt. Therefore, these solvates are difficult to desolvate, and when they do, the crystals collapse and recrystallize in a different form. These are named polymorphic solvates. In other cases, the solvent is not a crucial component of the infrastructure and only occupies the voids within the crystal. This way, the solvent molecules can be lost while not destroying the crystal, and these solvates are known as pseudopolymorphic solvates (2).

As the close-packing principle states, voids within the crystal lattice are unfavourable and the inclusion of solvent molecules provides strong interactions that help supporting and stabilizing the structure, allowing the solvate to form. In this sense, solvents with strong hydrogen bond donor or acceptor groups will offer interaction points with the drug that potentiate the crystallization. Solvent molecules can, in this way, fill cavities or channels created by the drug molecules, completing the close-packing arrangement and stabilizing the structure that otherwise would not assemble (3).

As both the conformation and chemical identities of each solvate differ from each other and from the anhydrous forms, they present distinct physicochemical properties (e.g. melting point and solubility) that can affect their pharmaceutical behaviour, which can be interesting from a product development point of view (2, 3). Nevertheless, even though solvates possess increased aqueous solubility most of the times, their utility may be limited by poor stability (due to desolvation) or potential toxicity of the solvent released during dissolution (3). It is not enough that the drug is released in the optimal amount from the pharmaceutical form. Toxicity and stability studies have to be performed to ensure that the product is safe, focusing in the full assessment of the drug's solid form during all the stages of processing and production, as several factors such as temperature, pressure and humidity may lead to structural transformations (3). For instance, form 2 of olanzapine was found to be metastable and considered unsuitable for commercial use due to its discoloration in the presence of air (5).

### **1.1.3. Amorphous Form**

The amorphous state is characterized by its lack of long-range arrangement and conformation. It is a solid state where the molecules are not organized in a repeated order, contrarily to what was seen with solvates and polymorphs (2, 6).

An interesting property is that the amorphous state does not have a well-defined melting point, due to its absence of a crystal lattice to break (6). In turn, it has a characteristic temperature point in which major transformations are observed. This referred as the glass transition temperature ( $T_g$ ) in which a brittle structure becomes rubbery due to the improved mobility of its molecules (6). This property can be modulated by the addition of plasticizers that improve the mentioned mobility, thus, reducing the glass transition temperature.

The amorphous state, due to its disorganized structure, possesses higher free energy. Therefore, it has the advantage of having higher apparent solubility and dissolution rates, which consequently offers enhanced bioavailability (7). On the other hand, it is also more physically and chemically instable and hygroscopic, which represent important challenges during product development and production (6, 7).

#### 1.1.4. Solid Dispersion

A strategy to stabilize, alter the solubility and the dissolution rate of some solid drugs is to incorporate them into a water-soluble matrix. This is, to formulate a solid dispersion, in which the solute and solvent crystallize together and form a homogeneous one-phase system (2). Teja *et al.* in their review article divided the solid dispersion into three classes: eutectic systems, solid solutions and microfine crystalline dispersions, depending on the distribution of the solute molecules in the surrounding solvent matrix (7).

There are several available excipients used to stabilize crystalline and amorphous drugs. In this study, special emphasis will be placed on water-dispersible polymers. Further detail about the theoretical aspects of water-dispersible polymers is provided in Section 1.4.

## 1.2 Solid State Characterization

The innovation in the field of characterization methods is remarkable, as new techniques and equipment continually arise with improved sensitivity, efficiency and reproducibility. This section provides an overview of the analytic techniques used in this work, that are useful for solid state characterization of a substance.

To have a more detailed explanation of theoretical aspects, further reading of references named in table 1 is advisable.

**Table 1** Methods used in solid state characterization.

	Method			References
Electromagnetic methods	Vibrational Spectroscopy	Absorption Spectroscopy	Fourier Transformation-Infrared (FT-IR),	(8-10)
		Scattered Spectroscopy	Raman Time-Gated Raman CARS	(8-15)
	Microscopy		Polarized Light Microscopy	(16)
		Scanning Electron Microscopy		
Thermodynamic methods	Differential Scanning Calorimetry (DSC) Modulated Differential Scanning Calorimetry (MDSC)			(3, 17, 18)

### 1.2.1 Spectroscopy

In a very simplistic way, a spectrometer is capable of detecting the characteristics of radiation that has been scattered, emitted or absorbed by atoms and molecules of a sample, according to the method used. These methods are based in the phenomenon produced when incident light interacts with a sample. Depending on the incident light's energy, the atoms and molecules can undergo rotational, vibrational or electronic transitions. With spectroscopy, it is possible to collect information regarding bond-identities, strengths, lengths and angles, and dipole moments (8).

Electronic states of a molecule are more spaced in energy-wise than vibrational states, which in turn have a larger gap of energy compared to rotational states. This means that electronic transitions require higher energetic radiation to occur (UV and visible region of the electromagnetic field). Vibrational transitions happen when infrared (IR) radiation is absorbed and, rotational transitions are a consequence of microwave absorption (9).

Emission spectroscopy detects the photon released when an electron returns to its lower energy state after being excited to a higher level of energy by an incident radiation. Characterizing the solid-state of a sample using emission spectroscopy is not very useful to study the structural aspects, thus it will not be explored in detail in this work. Absorption spectroscopy, in turn, has been gaining more and more attention in solid-state characterization, being one of the classic methods used.

#### 1.2.1.1 Absorption Spectroscopy

The theoretical fundamentals of spectrometry are complex and difficult to summarize, involving electromagnetism, optics and quantum-mechanical treatment. However, the experimental techniques for absorption spectroscopy in the UV, visible and IR region share some similarities. There is an incident beam that hits the surface of the sample and a reference beam that does not pass through the sample. The detector compares the intensity of the collected radiation with the intensity of the reference beam that did not interact with the sample (9). Hence, the detector measures the difference in the intensity between the incident light and the one that is emitted, i.e., the absorbed energy (8).

Bands in the mid-infrared (MIR), near-infrared (NIR) and Raman spectra are a consequence of molecular vibrations and, in turn, these vibrations are very sensitive to the structure of a molecule (10). The difference between these three methods is that while MIR and NIR-spectroscopies are absorption techniques, Raman spectroscopy is a scattering technique. Contrasting with scattering spectroscopy, mid- and near-infrared techniques use a disperse polychromatic incident radiation upon the sample, which in turn absorbs the specific vibrational frequencies of its molecules. Mid-Infrared techniques cover almost the same wavenumber region as Raman scattering ( $4000\text{-}400\text{ cm}^{-1}$  for MIR), while near-infrared covers the adjacent region, extending to visible wavenumbers ( $12500\text{-}4000\text{ cm}^{-1}$ ), thus, MIR captures the fundamentals of the vibrations, and NIR bands are a product of overtone and combination vibrations (10). Furthermore, typical range for a Raman setup is  $200\text{-}2000\text{ cm}^{-1}$ . Although, special setups can go to very low wavenumbers ( $10\text{ cm}^{-1}$ ) upto to about  $3200\text{ cm}^{-1}$  (as in TimeGated<sup>®</sup> Raman) or  $4000\text{ cm}^{-1}$  (as in Fourier transform Raman setups). In this project, Fourier-transform infrared (FTIR) spectroscopy with an attenuated total reflectance (ATR) attachment was used.

### 1.2.1.2 Scattered-Spectroscopy

#### Raman Spectroscopy

Raman spectroscopy explores vibrational transitions by measuring the frequencies present in the scattered radiation by a molecule. In this method, a monochromatic beam (between visible to NIR frequency region) irradiates the sample exciting the molecules to a virtual energy state above the vibrational quantic levels. At this point, three situations can occur: (a) the molecule returns to the ground energy level, emitting a photon with the same frequency as the incident light, thus lacking information in terms of molecular vibration (called Rayleigh effect, an elastic scattering); (b) the molecule returns to an energy state higher than the ground state, therefore emitting a photon with lower frequency than the excitation one (producing a Stokes line, an inelastic scattering); (c) or, lastly, the molecule's starting state is the first vibrational level and, therefore, when the molecule returns to a lower level (ground state), it emits a photon with higher energy than the incident one (known as Anti-Stokes radiation, also an inelastic scattering). In the last two phenomena, the difference between the incident and the emitted frequencies gives information about the vibrational energy absorbed which, once again, is very sensitive to the functional groups of a molecule (8, 10). Figure 1 illustrates the Raman scattering phenomenon, as well as the differences between fluorescence and resonance Raman scattering.

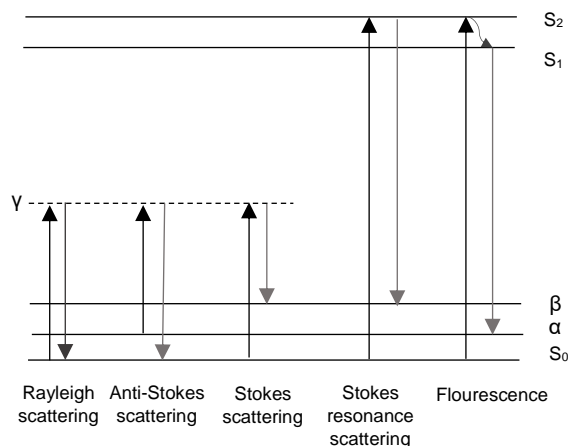


**Fig. 1** Diagram of Raman scattering phenomenon, alongside resonance and fluorescence effect.  $S_0$  represents the ground-state,  $S_1$  and  $S_2$  are two real energy states,  $\alpha$  and  $\beta$  are two real vibrational states and  $\gamma$  is a virtual vibrational state.

Regardless of the energy of an incident radiation, the photon-molecule collision may scatter the photon, i.e, change its direction of motion. Almost all the photons do not undergo energy changes (Rayleigh scattering), and approximately 1 in  $10^7$  actually lose some of its energy (Stokes line). This is one of the limitations of Raman spectroscopy, as the intensity of the scattered light is much lower than the incident beam ( $I_{\text{Raman}} \approx 10^{-4} I_{\text{Rayleigh}} \approx 10^{-8} I_{\text{source}}$ ) and, consequently highly sensitive equipment is required (8-10).

There is a complementarity between Raman and absorption methods from a structure-assessment perspective. For a Raman band to occur, there must be a change in the functional group polarizability, whereas in NIR and MIR there must be a change in the dipole moment. Hence, non-polar molecules are Raman active, while polar functions are infrared active (8, 10). Having said that, the symmetry of a molecule offers important clues to evaluate if a molecule is Raman or IR active. Symmetric stretch, for instance, tend to leave a dipole moment unchanged, while antisymmetric stretch has the tendency to have the opposite effect. Totally symmetrical vibrations are more likely to influence the polarizability, and thus, to be Raman active (8).

### Resonance Raman – Time Gate Raman

To overcome the difficulties related to the low intensities of the inelastic radiation in Raman, a modification of the basic method uses an incident beam of frequency close to the one needed to an electronic transition to happen (8). One of the consequences of using higher energetic radiation is that fluorescence can occur, overlapping with and sometimes completely masking the entire Raman spectrum. Instead of having narrow well-defined peaks, one obtains a single broad hill that lacks any useful information (14). For some molecules, the energy of the incident radiation can be enough to excite the valence electrons to the higher excitation level. The absorption phenomenon takes place in a femtosecond-scale, while the subsequent relaxation until it reaches the electronic lower level occurs in less than 100 ps. Afterwards, the valence electrons still need to return to the ground level of energy, which can be done by either the molecule emitting a new photon (fluorescence) or producing heating. On the other hand, Raman scattering takes place on the order of picoseconds (considered instantaneously). It is this difference in time that is the foundation of the TimeGated® technology, where a picosecond laser excitation font allied to a time-gated single photon counting array detector permits the capture of the instantaneous Raman scattering, while rejecting the delayed fluorescence (11, 14).

### Coherent Anti-Stokes Raman Scattering (CARS)

The other technique used in this work was coherent anti-Stokes Raman spectroscopy. This is a subtype of a Raman process that has been developed and gaining attention as the laser technology improves. It uses the coherence properties of two visible laser beams that are focused together in a sample. The resonance effect leads to an enhanced vibrational transition. By varying one of the frequency beams, it is possible to make the coherent scattered radiation matching the anti-Stokes frequency line, giving rise to a narrow beam of much higher intensity than the other Raman methods seen previously (8, 13).

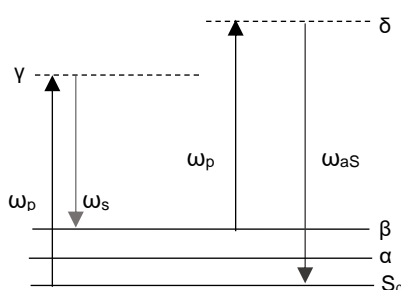


**Fig. 2** Diagram of the radiation frequencies and vibrational transitions involved in CARS process.  $S_0$  represents the ground-state,  $\alpha$  and  $\beta$  are two real vibrational states,  $\gamma$  and  $\delta$  are virtual vibrational states.

Figure 2 illustrates three real energy states ( $S_0$  represents the ground state, while  $\alpha$  and  $\beta$  are two vibrational levels) and two virtual states ( $\gamma$  and  $\delta$ ). The first pump (of frequency  $\omega_p$ ) impels the molecule to the virtual state  $\gamma$ , then through a photon tuned to a frequency  $\omega_s$ , the molecule returns to a lower energy state ( $\beta$ ). By the absorption of the second pump radiation (frequency  $\omega_p$ ), the molecule undergoes the transition to the higher virtual state  $\delta$ , allowing the emission of an anti-Stokes photon (frequency  $\omega_{as}$ ) as the molecule returns to ground energy state (12).

An interesting feature of CARS is the possibility of allying a spectral signal to a microscope and, hence, obtaining the chemical imaging of the sample. When coupled with the respective microscope, it becomes possible to capture the surface of a sample with the aim of investigating its morphology and homogeneity. By choosing a wavenumber where only one component is Raman active, it is possible to selectively visualize its presence and distribution

throughout the surface of the sample (19). Because of the high selectivity of this imaging technique, CARS is a very useful method in the solid-state characterization of a sample, making possible to image different components of a sample by changing the wavelength of the laser. Fussell *et al.* compared two imaging techniques (CARS and scanning electron microscopy) for the study of the distribution of drug particles on a carrier's surface, and revealed that the former identified clusters of the drug, while SEM only showed protuberances and did not clarify localised distribution of the drug on the surface (20).

## 1.2.2 Microscopy

### 1.2.2.1 Polarized Light Microscopy

This imaging technique combines physical, chemical and crystallographic data in one equipment. It is based on the optical properties of crystals, more specifically, the birefringence caused by different refractive index of a material. When a polarized radiation intersects an anisotropic sample, it is split into a slow ray (consequence of higher index) and a fast ray (result of lower index). Because of the different crystal's orientation (and sometimes, due to the presence of different polymorphs) in the sample, when the radiation reaches the viewer, an out-of-phase interaction is seen by the analyser as different colours (birefringence).

Most of the crystal structures are optically anisotropic, thus leading to birefringence when under polarized light. Conversely, materials lacking long-range structural order are more likely to be isotropic. This is a simple and direct tool to evaluate the presence of anisotropic materials and to have an insight clue of the sample's homogeneity (16).

### 1.2.3 Differential Scanning Calorimetry (DSC)

As explained previously, due to distinct crystal lattices, different polymorphs and solvates have different Gibbs free energy. The thermodynamic properties are, hence, very relevant for solid-state characterization, not only because they ultimately dictate the thermodynamic behaviour (thus, the physical stability) of a drug, but also because they inform about the polymorphic or the solvate form itself.

DSC studies the enthalpy changes (exothermal and endothermal events, as well as heat capacity changes) that a reference and a sample pan undergo when they are heated at a determined temperature rate. The DSC technique uses either a power compensation equipment, or a heat flux instrument. The power compensation equipment uses two furnaces – one for each pan – and the energy required for each pan to reach the same temperature is measured. The heat flux instrument has a single furnace where both the sample and the reference pan are heated and the difference in the heat flow output produced by the pans is measured (3, 17) The DSC profile is, therefore, the combination of the thermal behaviour of a compound when it is submitted to different temperature conditions. This includes melting, crystallization, boiling, dehydration, desolvation, glass transitions and polymorphic transitions – which are either endothermic or exothermic events (summarized in Table 2) (17).

**Table 2** Summary of the enthalpic transitions detected by DSC (17).

Endothermic Events	Exothermic Events
Fusion	Crystallization
Vaporization	Condensation
Sublimation	Solidification
Desorption	Adsorption
Decomposition	Chemisorption
Reduction	Solvation
Degradation	Decomposition
Glass Transition (a shift in the baseline)	Oxidation
Relaxation of glasses	Curing of resins

This thermodynamic method also informs about the relationship of the different polymorphs. In monotropic polymorphs only one of the polymorphs is the most stable at all temperature ranges, being the one with higher melting point and higher enthalpy of fusion. In enantiotropic polymorphs, in turn, there is a transition temperature where the stable form for a certain temperature condition becomes other rather than the previous polymorph (the most stable form for lower temperatures), and the polymorph with higher melting temperature has the lower enthalpy of fusion.

Another very interesting scope of this technique is the investigation of excipient-drug compatibility. Here, a 50% (m/m) physical mixture of the two components has to be prepared, in order to potentiate the interactions between both substances. In case of no interaction, the mixture's thermal profile should be the sum of each individual thermal properties. Otherwise, in cases where enthalpy of fusion is shifted, further analysis should be performed, to evaluate the nature and importance of that interaction (having in mind that an interaction does not necessarily mean incompatibility) (17, 21).

### Modulated differential scanning calorimetry (MDSC)

A very interesting extension of the DSC method is the application of a sine wave modulation to the temperature programme (instead of linear heating). Before going to further considerations about this method, it is important to remember the classification of thermal events as reversible or irreversible processes. While reversible processes are events that may be inverted when an infinitesimal variable is modified – in other words, the sample will absorb or radiate heat in order to match the surrounding temperature - an irreversible process is not in equilibrium with the programmed temperature, and therefore cannot be restored to the initial state, being a kinetically controlled process (18).

With MDSC it is possible to separate a linear heat flow signal dictated by the heat capacity, from a kinetically chemical event that undergoes at a certain temperature value – in simple DSC profile, in turn, it is seen a sum of both processes (17, 18). Thus, MDSC allows the investigation of overlapping events and complex transitions with greater resolution, the study of metastable melting phenomena and heat capacity data. A great advantage is, then, the separation of the glass transition temperature and the relaxation endotherm.

### 1.3 Solid Form of Olanzapine

Olanzapine is the name of the thienobenzodiazepine 2-methyl-4-(4-methyl-1-piperazinyl)-10H-thieno-[2,3-b][1,5]benzodiazepine molecule - an atypical antipsychotic drug used in the management of schizophrenia, bipolar disorder and other syndromes (5, 22). Fig. 3 illustrates the molecular structure of olanzapine.

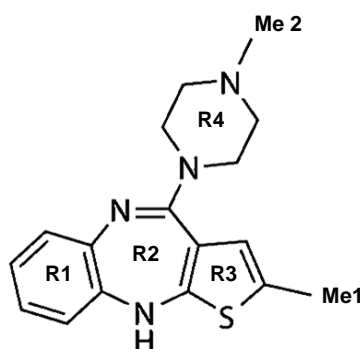


**Fig. 3** Molecular structure of olanzapine; In the present work, the benzyl ring is treated as R1, the azepine ring as R2, the thiophene ring as R3 and piperazinyl group as R4; Both methyl groups are numerated.

The olanzapine molecule is capable of H bonding through the nitrogen atoms, being one of them a H donor (the NH in R2) and two H acceptors (the other nitrogen of R2 and the nitrogen linked to Me 2 in R4). This nonpolar drug belongs to class II, according to the Biopharmaceutical Classification System, presenting low solubility and high permeability. It is a compound with more than 60 polymorphs registered in the Crystallographic Structure Database (CSD), having a diverse crystalline behaviour.

It was first developed by Eli Lilly and Company in 1996. In Portugal, it is commercialized as orodispersible tablets, regular tablets or coated tablets by several laboratories and brands.

### 1.3.1. Anhydrates of Olanzapine

Despite the existence of a multiplicity of crystal forms, it is well known from the literature that olanzapine has three stable anhydrates, form 1 being the most stable polymorph (22, 23). It should be noted that, initially, olanzapine's patent described the drug's polymorphs with roman numbers, and named form II the most stable form of olanzapine. The polymorph named form I in the initial patent was found to be metastable and was considered not suitable for pharmaceutical formulations, referring that form II was stable and, thus, "pharmaceutically elegant and, therefore, well adapted for commercial use" (24).

Despite this fact, the majority of authors in the literature refer to the most stable form as form I (or 1, in ordinal number), contradicting the original patent. Thus, this present document follows the last nomenclature, naming form 1 polymorph the most stable anhydrate of olanzapine. It should be noted that Reutzel-Edens *et al.* describe a third polymorphic anhydrate, but this one was refuted by Polla *et al.* stating that it seemed to be an elusive desolvation product, as it only has been obtained as a mixture of both polymorphs (form 1 and 2), and its structure is yet to be determined (4, 22, 23, 25). Thus, this form was not considered in this present work.

Olanzapine has two enantiomers that adopt mirror-related conformation. The interconversion happens by inversion of the diazepine ring (25). Reutzel-Edens *et al.* characterized in detail the solid-state and the structural relationship of form 1 and some of the hydrates of olanzapine. The two enantiomers of olanzapine appear to be packed in a centrosymmetric space groups dimer around an inversion centre. This symmetric dimer seems to be present in all solid forms of the drug, as it has been found in all different anhydrates and solvates (23, 25). Form 1 olanzapine is known to crystallize in a  $P2_1/c$  lattice, where the spatial complementarity between enantiomers drives the packing of the dimer, stabilized by van der Waals interactions between the complementary surfaces of the most stable conformational enantiomers. The C – H... $\pi$  is established between C22 – H...C9 and C22 – H...C4 (Fig. 4 a). Adjacent layers of dimmers appear to be linked through NH...H between N3 and N10 belonging to azepine ring R2 of neighbouring building blocks (Fig. 4 a) (25, 26). Because of this, each olanzapine molecule has one H donor and the two H acceptors available to interact with the surrounding molecules (25).



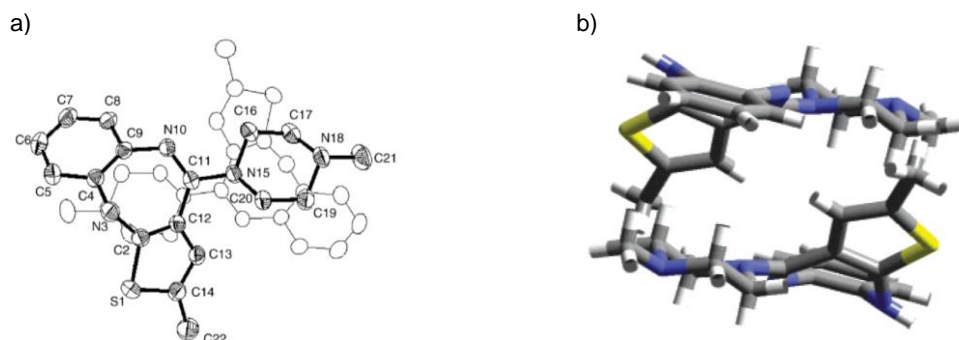


**Fig. 4** a) Molecular diagram of the olanzapine crystal building block (23); b) Crystal building block of olanzapine (25).

### Spectroscopic data

Regarding spectrophotometric data of olanzapine, Polla *et al* (23) divides the Raman spectra of olanzapine into four regions:

- Between 2700-3100  $\text{cm}^{-1}$  there is the contribution of many C-H groups (namely from benzene, piperazine, methyl, etc), where, by comparing form 1 and form 2 spectra, it would be possible to see some differences in certain peaks;
- From 1500 to 1700  $\text{cm}^{-1}$  there are bands corresponding to C-H and C-C links (explained in more detail further in this text).
- Between 600-1700  $\text{cm}^{-1}$  lies the *fingerprint* region. Here it is possible to find many information that can be used in the differentiation between the two forms.
- However, according to the authors, the best region to discriminate both polymorphs would be below 400  $\text{cm}^{-1}$ , where backbone deformations and lattice vibration are observed. Despite this suggestion, the range of the spectrum realized in the present work did not reach these wavenumbers, therefore this region was not considered in the description of the solid form of olanzapine.

This simplistic description is congruent with the work conducted by Ayala *et al.* (22) where a complete band assignment of the Raman and Infrared spectrum was made. According to the authors, the stretching vibration of the NH bond is visible at high wavenumbers. As expected, this band is intense in IR but not in Raman spectra. The fact that this band is shifted towards lower wavenumber confirms the hydrogen bond between molecules of olanzapine.

The authors attributed the bands between 1500-1600  $\text{cm}^{-1}$  to the double bonds C=C of benzene and thiophene groups, as well as to C=N of azepine ring. These bands appear partially coupled with NH and CH bending deformations. It is in this region that the most remarkable differences between spectrum of both forms are seen, and from where the present work was based to characterize solid form of olanzapine samples. Form 2 reveals a splitting of the peak at 1517  $\text{cm}^{-1}$  in Raman spectra, as well as a new infrared band at 1601  $\text{cm}^{-1}$  (22, 23) that are not seen in form 1 spectra.

Between 1300-1500  $\text{cm}^{-1}$  the overlapping bands correspond mostly to deformations of the methyl, methylene and C-H groups. Continuing to lower wavenumbers, from 1100-1300  $\text{cm}^{-1}$  the C-C and C-N stretching vibrations are predominant. Below this interval the bands are less complex and less overlapped. At 1043  $\text{cm}^{-1}$  it is visible the characteristic of the in-plan deformation of the benzene, and the infrared band at 745  $\text{cm}^{-1}$ , associated with the out of plane deformation of the CH bonds CH bonds of the same group. Finally, the vibrational modes corresponding to the lattice vibrations are visible at lower wavenumbers, and are highly sensible to the crystalline form, and thus, represent an important feature to discriminate the polymorph of olanzapine (22).

Ayala *et al.* also mention differences between both forms in the C-N and N-H stretching region, being the most relevant the  $19\text{ cm}^{-1}$  difference in the NH stretching band, and the half-band width (22). But, once again, the most notable variances are found in the region of the stretching vibrations of the double bonds. Here it is clear that, while form 1 has a well-defined single peak at Raman shift  $1517\text{ cm}^{-1}$ , form 2 reveals a two peaks band.

Ayala *et al.* provide a table with a compilation of the Raman shifts and wave numbers of each peak between  $748\text{--}1594\text{ cm}^{-1}$  and the respective band assignment. In this present work, a new table (Table 3) was produced with some interesting peaks according to the former works of Polla *et al.* (23) and Ayala *et al.* (22), considering the ones specially involved in H bond and the ones that were proposed by the previous authors as good differentiator bands.

One more band important to notice in the IR spectra is the one in  $3250\text{ cm}^{-1}$  in the case of form 1 and  $3269\text{ cm}^{-1}$  in the case of form 2. These correspond to the NH stretching mode of the R2 ring, which is worth noticing because of the possible deviations when an interaction is occurring.

### Thermal Studies

Polla *et al.* described form 1 and form 2 as a monotropic system, sustaining this statement with DSC diagrams of form 1 and 2. Form 1 shows an endothermic peak corresponding to the melting of olanzapine with a  $T_{\text{onset}}$  of  $194^{\circ}\text{C}$ , and a latent heat of approximately  $143\text{ J/g}$ . Form 2, in turn, also reveals a second endothermic peak with a  $T_{\text{onset}}$  of  $177^{\circ}\text{C}$  and, right after it, an exothermal event overlapping the first one (23). The authors provide an energy vs temperature diagram and illustrate the differences in the Gibbs energy that drive the transformation between the two forms. The conclusion is that the energy barrier between form 1 and 2 is high enough to prevent the conversion between forms.

#### **1.3.2 Methanolate**

In this present project, methanol was used as a solvent with the aim of solubilizing all the compounds (drug and polymers), and produce a final polymeric film (by solvent casting). Thus, it becomes important to consider the possibility of the formation of a solvate in the final product.

As previously described in the literature, olanzapine is highly capable of forming solvates with a vast variety of solvents. Cavallari *et al.* classified the solvents into four categories according to their capacity to form solvates or anhydrous forms of olanzapine: solvents that do not form solvates with olanzapine, leading to crystallization of only form 1; those capable of forming a solvate and leave form 1 after desolvation; those also capable of originate a solvate and leave, in turn, an indication of a presence of form 2 in the thermogram; and those capable of form a solvate, but where the presence of form 2 is not proeminent. Methanol fits into those that form a solvate and leave form 1 after desolvation (5). Polla *et al.* also refer that the anhydrates can be obtained from the desolvation of different hydrates and solvates, which suggests that all solid forms have a common packing arrangement. This appears to be the case, regardless of the solvent used (23). In this topic, Bhardwaj *et al.* provide an extended characterization of solvates and its space groups, where it is possible to visualise that the majority of solvates have  $P2_1/c$  space group, including olanzapine methanolate, corresponding to the space group of olanzapine anhydrates, which is congruent with the widespread statement that there is a common packing arrangement (4).

Wawrzycka-Gorcyca *et al.* characterized the intermolecular interactions between host and guest molecules, concluding that olanzapine dimers form channels where methanol occupies the voids linking neighbouring columns. Specifically, strong hydrogen bonds are made through  $N_{\text{host}} - \text{H}\cdots\text{O}_{\text{guest}} - \text{H}\cdots\text{N}_{\text{host}}$  of azepine ring N3 piperazine ring N18 (Fig. 4 a) (26).

To the best of our knowledge, there is no spectroscopic information of olanzapine's solvates in the literature.

## Thermal Studies

In data concerning thermodynamic events in DSC, it is possible to find different temperature ranges for the desolvation process in the literature (from 70 – 130 °C). Previous studies described the thermic events of several solvates with different crystallization conditions, and found three persistent features: a) between 110-120 °C a first endotherm is visible followed by an exotherm event – corresponding to the phenomena of desolvation and recrystallization, respectively; b) an endothermic event at 197 °C congruent with melting of form 1 olanzapine; c) and finally, the stoichiometry of the solvate is 1:1 (determined by TGA). Moreover, the conclusion in different studies is that the processes of desolvation depends on the crystallization conditions, even though the stoichiometry of the solvate is 1:1 irrespective of the conditions used for crystallization (5, 26).

Form 1 appears to be the final form into which the solvates transform. Moreover, when the samples were left in the desiccator at room temperature for 2 weeks, there was a complete loss of the solvent, so that only form 1 was found, according to different studies (4, 5, 27).

### **1.3.3 Amorphous Form**

With respect to product development, an amorphous state of an active ingredient could offer the advantage of having higher bioavailability (as consequence of its enhanced solubility and dissolution rate) and, structure wise, more uniformity throughout the product, comparing to when the drug is in a polymorphic form.

The amorphous form of olanzapine was found to have a  $T_{g\text{onset}}$  close to 66 °C, according to the amorphous form in the patent of the drug (28). Bhardwaj *et. al* found similar results with a  $T_g$  nearly at 70 °C (4). Additionally, no other relevant event is visible in a range of 55-110 °C, and olanzapine crystallizes into form 2 near 108 °C. This high temperature of transition is very interesting and suggests that amorphous form could be compatible with product development, because it would be stable at room temperature (25°C) during the product's shelf life (28). A IR spectrum of amorphous olanzapine is presented in the patent of the drug (28). However, to the best of our knowledge, the exact characteristic peaks of amorphous olanzapine are not known.

## **1.4 Polymers**

In contrast with what has been seen previously for crystalline compounds, some molecules are excessively large and flexible and it becomes difficult to align and ensure a crystalline conformation. This occurs with polymeric materials, which are described as semicrystalline compounds due to its ordered regions surrounded by- disordered parts that do not allow a total crystal structure to assemble. This feature affects the material properties and, ultimately, the performance of the pharmaceutical product (6). Due to the multiple intra- and inter -chain cross links possibilities, and its consequent complex conformation, polymers provide a suitable network structure that interferes with the mobility of the drug, thus, creating a solid dispersion and stabilizing the drug solid state (7).

### **1.4.1 HPMC**

Hydroxypropyl methyl cellulose (HPMC) is a widespread polymer used in both solid and liquid pharmaceutical forms, it is adequate for internal or external usage, and can act as bioadhesive material, coating or controlled release agent, emulsifier, stabilizer, thickening agent, amongst other functions. The amount of methoxy and hydroxypropoxy groups defines the commercial grade of the compound, and influences the viscosity of the environment where it is used. It has a molecular weight between 10 000 – 1 500 000 (29). Figure 5 depicts the molecular structure of the polymer.

It is a non-ionic polymer, thus being suitable for oral administration. The functional groups present in the side chains of the molecule provide approximately 10-17 H-bond donors and 0-7 acceptors per monomer unit (7, 30).

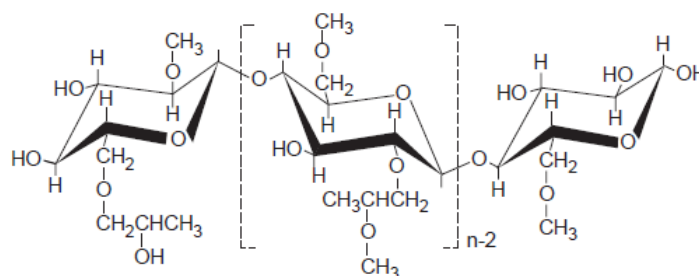


**Fig. 5** Molecular structure of HPMC.

Within the scope of this work, HPMC was used as a film-forming excipient, since it has been one of the most frequently used materials for this purpose (31-33). Regarding its physico-chemical properties, it is soluble in cold water, in methanol, dichloromethane, and mixtures of water and alcohol. In contrast, it is insoluble in hot water, chloroform, and ethanol (95%). HPMC has a glass transition temperature around 170-180 °C and browns at 190-200 °C (29).

With regard to the IR spectra of HPMC raw material, one important feature is the band at 3460  $\text{cm}^{-1}$ . This was assigned as the stretching vibration of hydroxyl groups of the polymer by Zheng *et al.*, which are thought to be responsible for the interactions with other substances (34).

#### 1.4.2 Soluplus®

Soluplus® is the commercial name of polyvinyl caprolactam-polyvinyl acetate-polyethylene glycol copolymer (PCL-PVAc-PEG), which was first designed to improve the solubility of solid dispersions constituted by poorly water-soluble drugs. It has a molecular weight of approximately 90 000-140 000, it is water soluble and it has a glass transition temperature around 70 °C. It is amphiphilic, having three H-bond donors per monomer unit (35, 36). Soluplus® has the potential capacity to act as matrix former and solubilizer of the drug, and different approaches have been used for the development of solid dispersions of poorly water soluble drugs using this polymer (19).

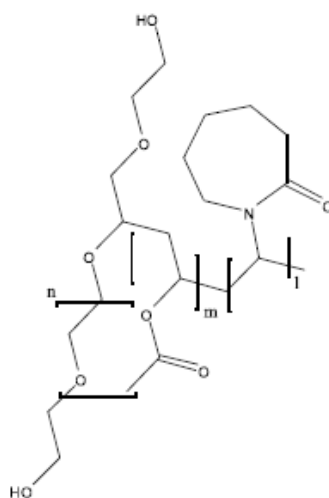


**Fig. 6** Molecular structure of Soluplus.

The IR spectra of Soluplus presents important peaks at 2920, 2850, 1750 and 1650  $\text{cm}^{-1}$ . In the stretching region of the spectra, it is possible to observe the bands corresponding to the

CH vibration modes between 3000-2850  $\text{cm}^{-1}$  (seen in Fig 10 c). Continuing to lower wavenumbers, at 1725  $\text{cm}^{-1}$  it is possible to visualise the vibration of the ester group ( $\text{OC(O)CH}_3$ ), while at 1625  $\text{cm}^{-1}$  the amide groups (CON) become prominent. Between 1500-1000  $\text{cm}^{-1}$  there are NH bending vibration, as well as COC stretching vibrations (37).

### 1.5 Gap in the literature

Previous studies have been studying the solid-state of olanzapine within solid dispersions obtained with different techniques, for instance via hot-melt extrusion (38). Additionally, different studies include a drug-excipient compatibility study with a wide variety of polymers. Peres-filho *et al.* (21) presented a study regarding the compatibility of olanzapine with excipients typically used in solid oral pharmaceutical forms, where a thermoanalytical assessment was performed. Even though the results are interesting aiming a pharmaceutical formulation development, neither HPMC nor Soluplus were used, thus not providing insights on the usage of these polymers.

## 2. Aim

The aim of this study was to characterize the drug-polymer compatibility and the solid state of olanzapine in a polymeric orodispersible matrix as a primary stage of product development.

## 3. Materials and Methods

The following materials were utilized: Olanzapine (Commercialized olanzapine, Batch 019-120702), HPMC (Methocel® E5 Premium EP, Batch MG09012N21), Soluplus® (BASF, lot 71013547G0), Methanol (VWR Chemicals Prolab, HiperSolv Chromanorm, Batch 16Z1356).

With the aim of characterizing the solid form of commercial olanzapine, an in-depth comparison of the spectroscopic results of the raw material with the ones presents in previous works was made. Then, an estimation of the olanzapine's solubility in methanol was performed. A saturated solution of olanzapine was prepared and screened in a UV spectrophotometer, then, a calibration curve was used in order to calculate the concentration of the solution. Afterwards, films of olanzapine were produced by solvent-casting technique in which methanol was used as solvent with the aim of solubilizing both olanzapine and the polymers. Primary solutions of olanzapine-polymer were prepared in a concentration of 1:1 (m/m %). In order to study possible interactions between olanzapine-HPMC and olanzapine-Soluplus, physical-mixtures of drug-polymer were prepared and submitted to the same analysis than the films. An attempt of characterizing the solid state of the drug in the final product, as well as possible interactions between the polymers and the drug, were made. In this sense, spectroscopic screening and thermodynamic analysis were performed, to which FTIR, Raman, TimeGated as well as CARS spectroscopy and DSC analysis were made.

### 3.1 Solubility Analysis

For the preparation of a primary saturated solution of olanzapine, an amount of 20 mg of the drug was added to 100 mL of methanol and let to dissolve in a rotary shaker for 48h at 25°C. Three aliquots were diluted in order to screen them in a UV spectrophotometer, and a wavelength of 264 nm was chosen to the analysis. A calibration curve was calculated with seven appropriate concentrations. And the solubility was determined with a filtrated aliquot of the sample. All measurements were performed three times (39).

### 3.2 Preparation of the samples

The physical mixtures were produced by mixing the drug and each polymer in a proportion of 1:1 (m/m) in a mortar. The mixture (500 mg) was transferred to an Erlenmeyer. The solvent

was added (10 mL), and the system was led to dissolve by stirring under magnetic conditions overnight. The solution was casted in a Teflon plaque with a casting device, and the solvent was led to evaporate at room condition in the laminar air flow workstation for 4 hours. The obtained films were wrapped in aluminium foil and stored in a vacuum desiccator for further measurements.

### 3.3 Polarized Light Microscopy

Samples of olanzapine powder and fresh made films were observed under polarized light in order to explore the possible presence of crystals in the samples.

### 3.4 Spectrophotometry

IR spectra were recorded with Fourier Transform Infrared (FTIR) spectrometer with attenuated total reflection (ATR) accessory. Spectra collected within a range between 4000 and 650  $\text{cm}^{-1}$ , were acquired by accumulating 64 scans at a resolution of 4  $\text{cm}^{-1}$ .

Raman spectra were acquired in a Kaiser Raman Spectrometer (Raman RXN Systems), in a range of 500-1950  $\text{cm}^{-1}$ . For calibration of the equipment, cyclohexane was used.

Time-resolved Raman spectrum of olanzapine, HPMC and Soluplus raw materials were recorded with a TimeGated<sup>®</sup> device. A picosecond pulsed laser source (MOPA microchip-based; 532 nm) with pulse width < 100 ps was used, and complemented with detector CMOS-SPAD array chip with 128x8 active elements. The spectral resolution was 10  $\text{cm}^{-1}$ , and the Raman shift range was from 264-3100  $\text{cm}^{-1}$ .

CARS imaging was recorded using a pulsed laser (Nd:YVO<sub>4</sub>) which fundamental wavelength was frequency doubled to pump an optical parametric oscillator (OPO, APE GmbH, Germany) that produced two dependently tunable laser beams. The fundamental beam was combined with one of the beams from the oscillator and directed into an inverted microscope equipped with a laser-scanning confocal scan-head and photomultiplier tube (PMT) and GaAsP hybrid (HyD) photodetectors. The chosen wavenumber to perform spectral imaging was 1517  $\text{cm}^{-1}$ .

### 3.5 DSC

Differential Scanning Calorimetry was performed in a Mettler Toledo with a dry N<sub>2</sub> purge gas, the flow used was 50 mL/min, with a heating rate of 10 °C/min. The temperature range scanned was 25-200°C, and the measurements were performed in aluminium crucibles.

### 3.6 Data Analysis

Macroscopic features as peeling from Teflon plaque, flexibility, brittleness/resistance and colour of the obtained films were qualitatively characterized and compared.

Spectrophotometric data was exported to Origin 9.0 software, and the baseline corrections of Raman spectra were performed according to Savitzky-Golay method. CARS imaging was obtained using the LAS X<sup>®</sup> 3.0.2.16120 software provided by Leica Microsystems<sup>®</sup>.

## 4. Results

### 4.1 Solubility Analysis

With the equation 1 it was possible to measure concentration of olanzapine in a methanol solution.

$$y = 48.73 x + 0.0134$$

*Eq. 1* Calibration Curve - Concentration vs Absorbance ( $R^2= 0.9993$ );

Equation 1 found that near 1.0929 mg of olanzapine can be dissolved in one mL of methanol (1.0929 mg/mL;  $\sigma=0016442$ ;  $n=3$ ).

### 4.2 Observational characterization of fresh made film

Regarding the polymeric films only containing 100% of each polymer, some differences were noted between HPMC and Soluplus. HPMC was much more viscous and difficult to dissolve than Soluplus. Soluplus, in turn, showed to be the opposite of Methocel, as it was very easy to dissolve in the same volume of solvent, and did not grant viscosity to the final solution. Because of the usage of the casting device, a viscous solution was desirable, therefore, the viscosity conferred by HPMC was an advantage offered by this polymer. HPMC film was very easy to peel from Teflon plaque, being flexible and maintained its integrity. Conversely, Soluplus film was very brittle and its removal from the plaque had to be handled very carefully. These characteristics of flexibility were aggravated with the adhesion of olanzapine. As a result, none of the drug-polymer films were removed intact from the Teflon plaque. This feature is thought to be improved by altering the method, using a Petri dish instead of a Teflon plaque for casting the solution. In this way, the resulting film could be thicker as a Petri dish would be capable of holding a higher volume of solution and, hence, when the solvent vaporizes, it could leave a film with higher integrity and resistance. Comparing to the films made entirely of polymer, the lack of resistance of olz-polymer films could be explained with the presence of olanzapine crystals within the matrix net, which hinder the cross-link between side chains of the polymer.

As depicted in Figure 7 all obtained films were opaque, and the ones containing olanzapine gained a yellow coloration (Fig. 7 from c) to e)).

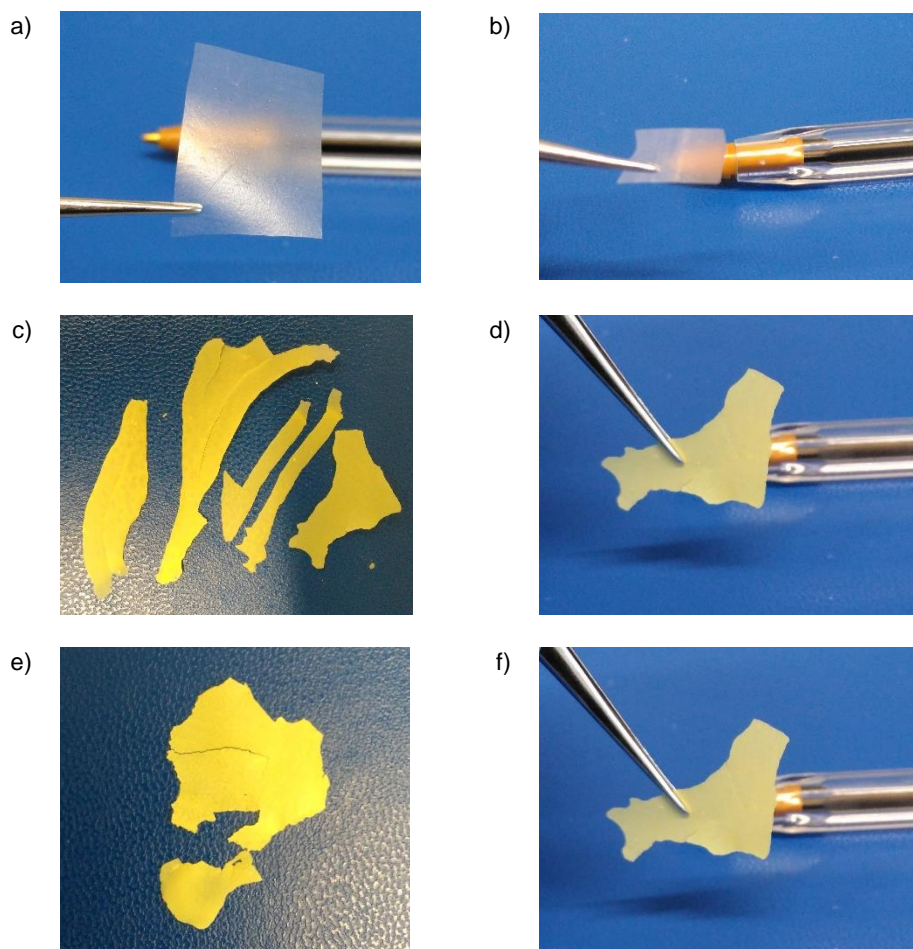


**Fig. 7** Obtained films containing: a) HPMC film (100% polymer); b) Soluplus film (100% polymer); c) HPMC-Olz film (50% m/m Polymer-Drug); d) HPMC-Olz film (50% m/m Polymer-Drug); e) Soluplus-Olz film (50% m/m Polymer-Drug); f) Soluplus-Olz film (50% m/m Polymer-Drug).

Quantitative measurements of flexibility, as tensile strengths and peeling, were beyond the scope of this work. Nonetheless, proportions of less percentage of olanzapine would improve the sensorial features described above, as a thicker (thus stronger) matrix would assemble.

### 4.3 Polarized Light Microscopy

In a first approach, the polarized light microscopy revealed some refringence, which means that there were crystals present in the polymeric matrix. It is also visible that the drug does not seem uniformly disperse in the matrix (Fig 8). The presence of crystals was expected, since the concentration of olanzapine in the casted-solution was much higher than the concentration of the solution described in section 4.1. Nonetheless, it is known that HPMC and Soluplus offer enhanced solubility to poor soluble drugs (through micelle formation), thus allowing a higher amount of olanzapine to dissolve in the solution. This way, crystals were expected, but neither the dispersion nor the size of the crystals were predictable.

One interesting parameter to study would be the time of dissolution and its influence on the dispersion of the crystals.



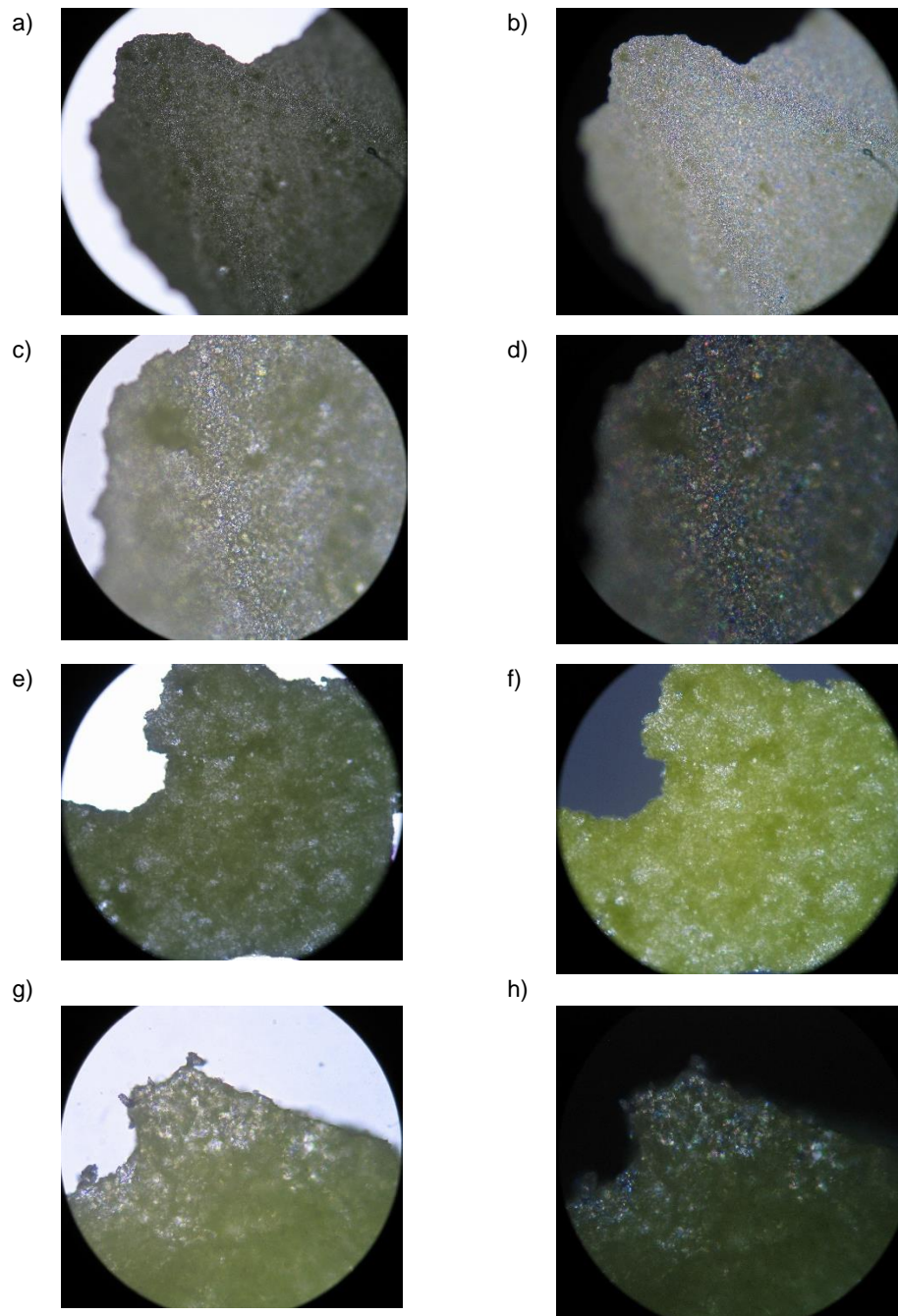


**Fig. 8** a) HPMC-Olz Film; Amp. 10x; b) HPMC-Olz Film; Amp. 10x; c) HPMC-Olz Film; Amp. 40x; d) HPMC-Olz Film; Amp. 40x; e) Soluplus-Olz Film; Amp. 10x; f) Soluplus-Olz Film; Amp. 10x; g) Soluplus-Olz Film; Amp. 40x; h) Soluplus-Olz Film; Amp. 40x.

## 4.4 Spectroscopic Characterization

### 4.4.1 Starting Materials

Figures 8 and 9 show the obtained Raman and IR spectra of olanzapine, HPMC and Soluplus raw materials. Fig. 9 b) represents a zoom-in of the Raman spectra, focusing in the four chosen characteristic peaks of olanzapine. As stated before, Table 3 compiles the Raman shifts and wavenumbers between  $748\text{--}1594\text{ cm}^{-1}$  and the respective band assignment proposed by Ayala *et al.* In this present work, an additional column was produced with the observed peaks. Thus, a simple comparison with the previous works was made. Special attention was given to the ones involved in H bond and the ones that were proposed by the previous authors as good differentiator bands.

Regarding HPMC curves, it is noticeable that the signal is quite weak, originating from mild bands. In the IR spectrum (Fig. 9 c) a mild band is visible at  $3460\text{ cm}^{-1}$ , where the stretching vibrations of the polymer's OH groups occur. Finally, the Soluplus' IR curve (Fig. 10) shows the characteristic peaks presented before,  $1650$ ,  $1750$ ,  $2850$  and  $2920\text{ cm}^{-1}$ . One can verify the presence of the explained groups in section 1.4.2 of this work.

Once characterized the raw materials, it is possible to compare this spectrum with the ones obtained with the physical mixtures as well as the produced films. A detailed analysis and discussion of the results is made in the following chapter (Chapter 6).

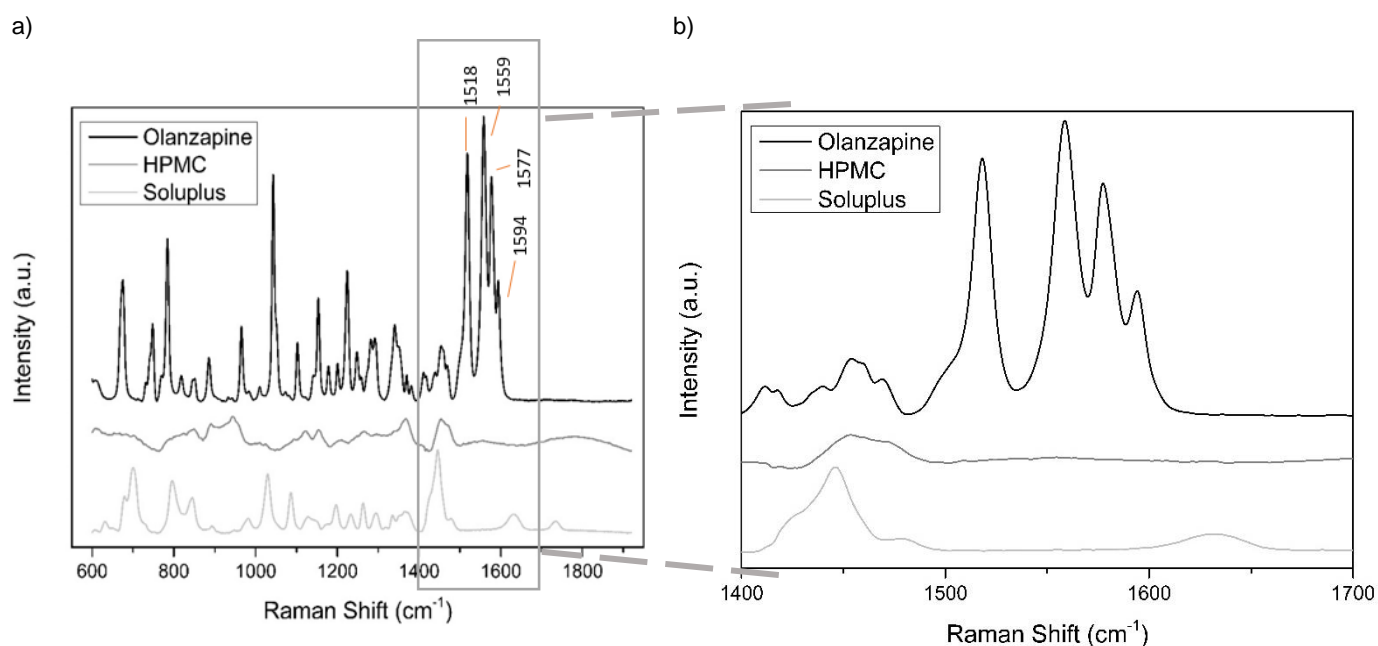


**Fig. 9** Raman spectrum of Olz, HPMC and Soluplus Powder: a) full spectra; b) Raman shift  $1400\text{--}1700\text{ cm}^{-1}$ .

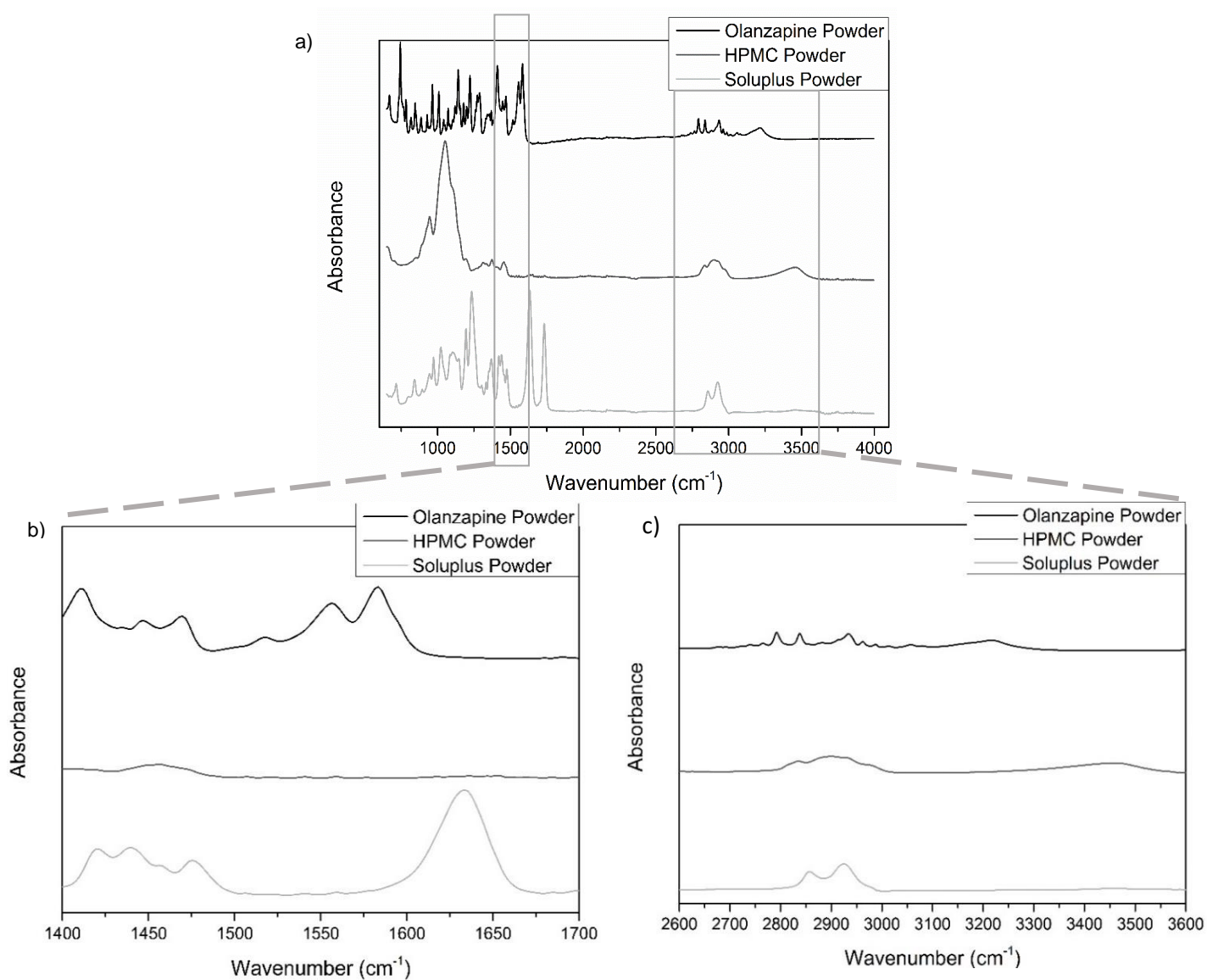


**Fig. 10** ATR IR spectrum of Olz, HPMC and Soluplus powders: a) full spectra; b) 1400-1700 cm<sup>-1</sup> and c) 2600-3600 cm<sup>-1</sup>.

**Table 3** List of olanzapine's peaks of interest, produced according to Ayala's work and the obtained spectrum.

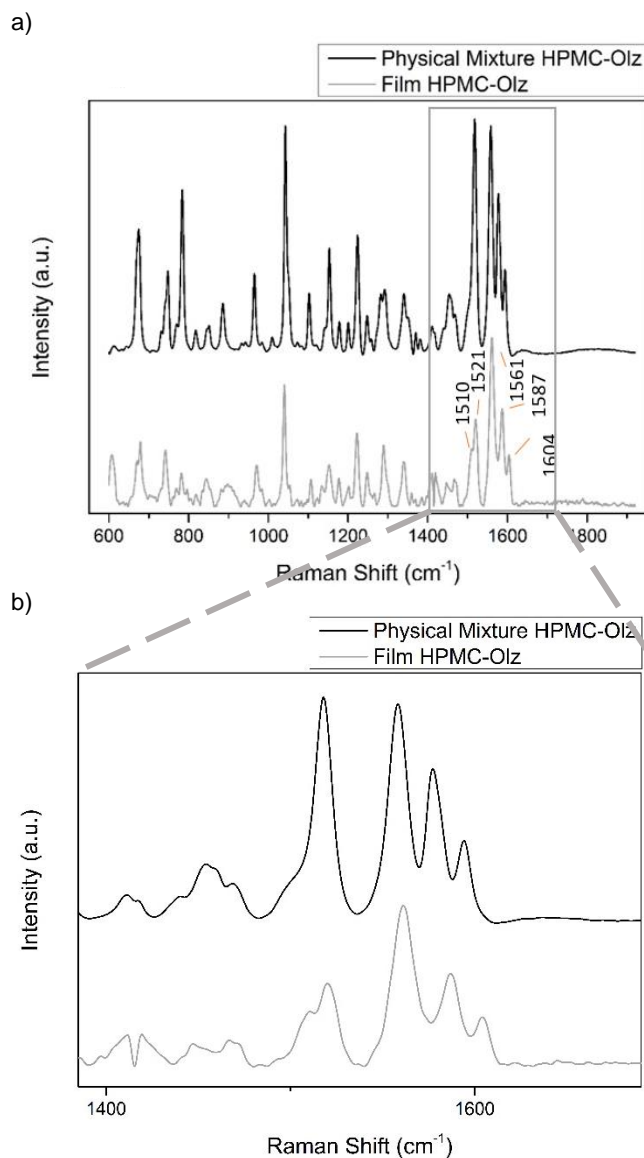
Previous Work (22)				Observed in the present work						Assignment
Form I		Form II		Olz Powder		Polymer-Olz Film				
Raman	IR	Raman	IR	Raman	IR	HPMC		Soluplus		
						Raman	IR	Raman	IR	
1594	1593	1600	1601	1594	-	1604	-	1603	-	<b>R1 [8a], R2 CN stretching</b>
-	1584	1586	1589	-	1583	1587	1586	1588	2586	<b>R1 [8a], R2 CN stretching + NH deformation, R3 CC stretching</b>
1577	-	1580	1582	1578	-	-	-	-	-	<b>R2 NH deformation + R3 CC stretching + Me<sup>1</sup> CH<sub>3</sub> deformation</b>
1558	1558	1559	1559	1559	1556	1561	1560	1562	-	<b>R1 [8b], R2 CN stretching, R3 CC stretching + CH deformation</b>
1517	1516	1522	1523	1518	1518	1521	1521	1520	1515	<b>R2 NH deformation, R3 CC stretching + Me<sup>1</sup> CH<sub>3</sub> deformation</b>
1499	-	1509	1508	-	-	1510	-	1509	-	<b>R1 [19b], R2 NH deformation</b>
1445	1448	-	1443	-	1447	1447	-	1447	1446	<b>R4 CH<sub>2</sub> deformation</b>
1435	1435	-	-	-	1435	-	-	-	-	<b>R1 [19a], R2 NH deformation + Me<sup>1</sup> CH<sub>3</sub> deformation</b>
1419	1420	1423	1426	1417	-	1420	-	1421	-	<b>R4 CH<sub>2</sub> deformation+ Me<sup>2</sup> CH<sub>3</sub></b>
1411	1412	1417	1418	1412	1411	1410	1414	1411	1412	<b>Me<sup>1</sup> CH<sub>3</sub> deformation</b>
1382	-	1382	1381	1381	1380	1385	-	1385	-	<b>R1 [19a], R2 NH deformation</b>
1377	1379	-	-	-	-	1376	-	-	1379	<b>R4 CH<sub>2</sub> wagging + Me<sup>2</sup> CH<sub>3</sub> deformation</b>
1370	1369	1366	1365	1370	1369	1369	1368	1368	1368	<b>R2 CC stretching + NH deformation, R4 CH<sub>2</sub> wagging, (R2)CN(R4) stretching</b>
1353	1352	-	-	1350	-	-	-	-	-	<b>R4 CH<sub>2</sub> wagging</b>
-	1271	1269	1269	-	1272	1266	1266	1265	-	<b>R1 [3], R2 CN stretching, R4 CN stretching</b>
1248	1247	1251	1253	1248	-	1248	-	1249	-	<b>R1 [3], R2 NH deformation + CN stretching, R4 CN stretching + CH<sub>2</sub> twisting</b>
1224	1223	1221	1221	1224	1222	1223	1221	1222	1222	<b>R1 [18b], R2 (ring) stretching, R4 CN stretching + CH<sub>2</sub> twisting</b>
-	-	1190	1190	-	-	-	-	1187	-	<b>R2 CN stretching, R3 CH deformation + CC stretching</b>
1154	1155	1157	1157	1154	1155	1153	-	-	-	<b>R4 ring stretching + CH<sub>2</sub> twisting + Me<sup>2</sup> CN stretching + CH<sub>3</sub> rocking</b>
-	1152	1150	1150	-	-	-	-	1151	-	<b>R4 (ring) stretching + CH<sub>2</sub> twisting, Me<sup>2</sup> CN stretching + CH<sub>3</sub> rocking</b>
1142	1143	-	1142	1142	1142	-	1146	-	1144	<b>R4 (ring) stretching + CH<sub>2</sub> twisting, Me<sup>2</sup> CN stretching + CH<sub>3</sub> rocking</b>
1103	1102	1105	1105	1103	1104	1107	1105	1107	1105	<b>R1 [18a], R2 CN stretching, R3 CH deformation</b>
965	965	973	971	965	964	970	969	970	968	<b>R2 (ring) deformation, R3 CS stretching, R4 (ring) twisting</b>
-	934	-	935	933	-	-	939	935	935	<b>R4 (ring) deformation + CH<sub>2</sub> rocking, Me<sup>2</sup> CH<sub>3</sub> rocking</b>
886	887	902	904	886	887	907	-	903	905	<b>R1 [12], R2 (ring) deformation</b>
						898			888	
819	817	816	817	818	818	819	821	819	819	<b>R2 (ring) deformation, R3 (ring) deformation, R4 CN stretching</b>
-	813	-	832	-	-	-	-	-	-	<b>R1 [6b], R2 (ring) deformation + NH out-of-plane bending, R3 CS stretching, R4 CN stretching</b>
748	745	761	757	748	745	759	-	740	745	<b>R1 [11]</b>

Notes: The benzene moiety modes are labelled according Wilson's notation, preserving the previous author's description.

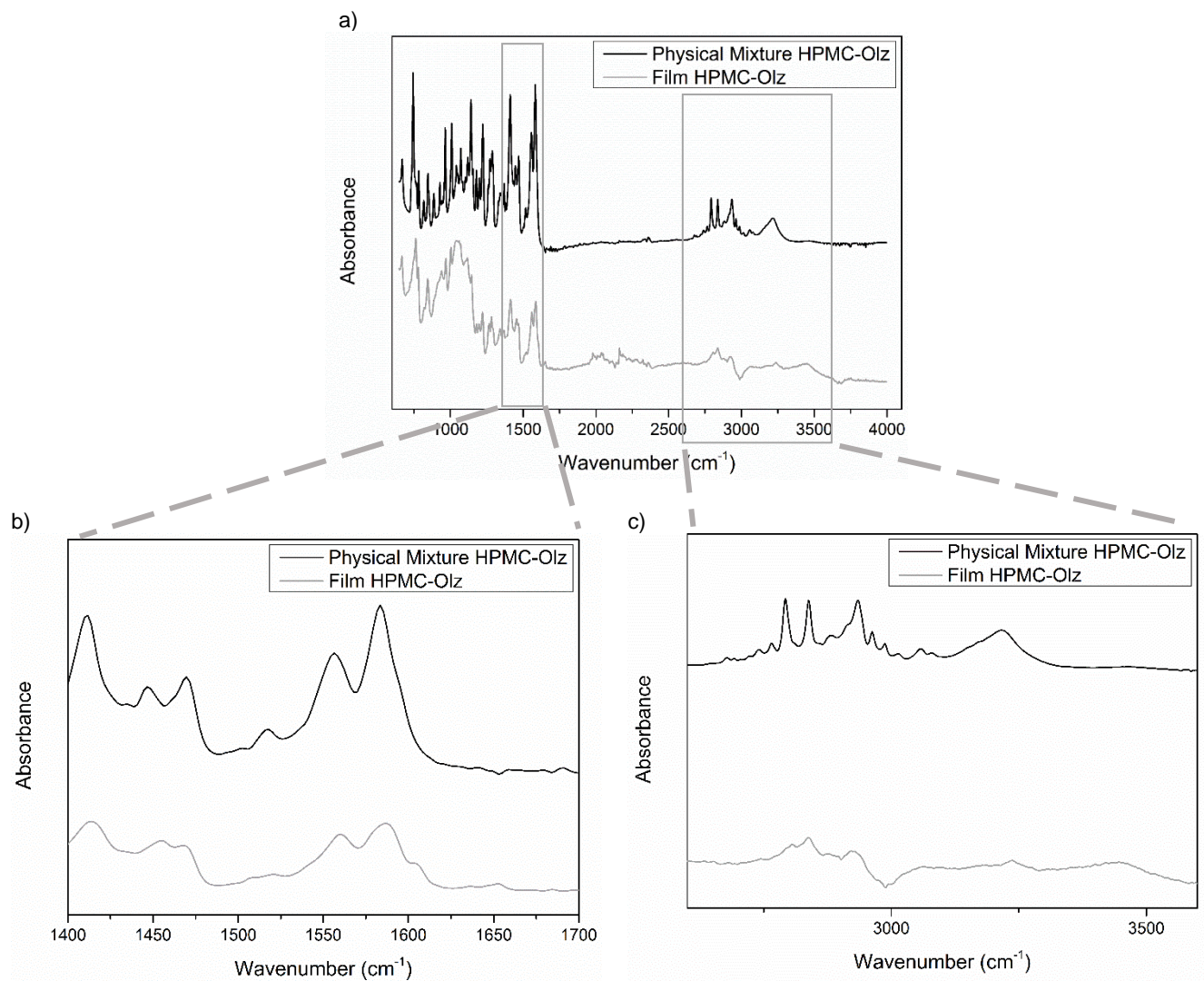
#### 4.4.2 Physical Mixtures and Films

##### HPMC-Olanzapine

The Raman and IR spectra obtained from the HPMC – Olz physical mixtures and films are presented in Figures 11 and 12. Key changes are noticeable between the spectra of the raw materials and the one of the produced films. Table 3 compiles the main interesting peaks, where several differences are visible in the Raman shifts, as well as in the wavenumbers of some peaks that would be present in the case of the pure drug.



**Fig. 11** Raman spectrum of HPMC-Olz physical mixture and film: a) full spectra; b) Raman shift 1400-1700 cm<sup>-1</sup>.



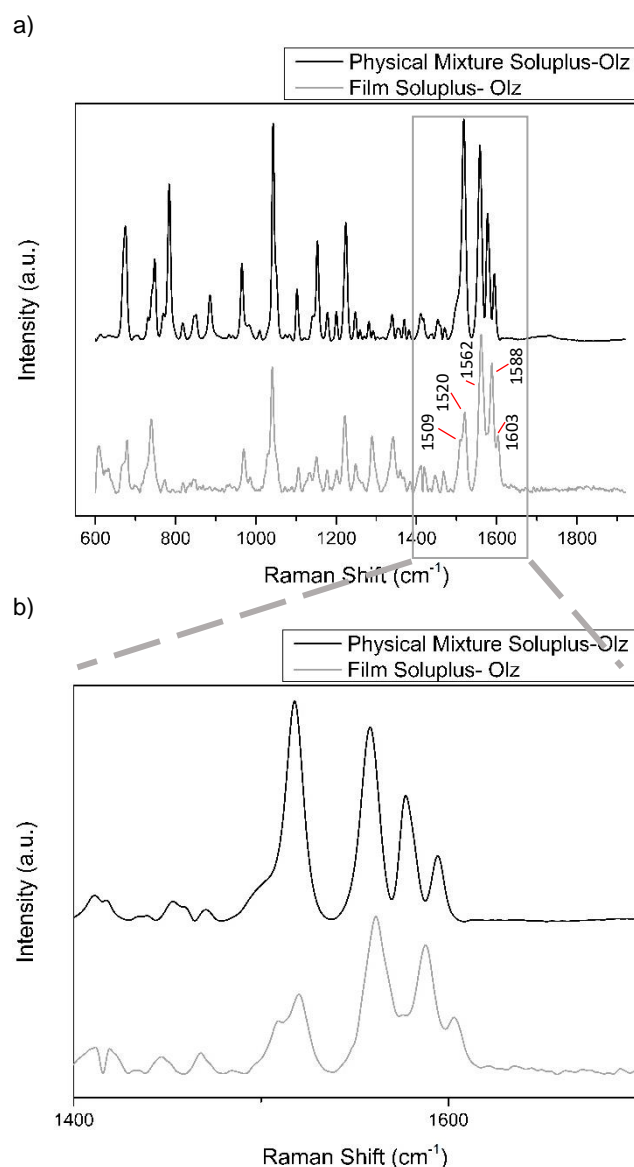
**Fig. 12** ATR IR spectrum of HPMC-Olz physical mixture and film: a) full spectra; b) 1400-1700  $\text{cm}^{-1}$  and c) 2600-3600  $\text{cm}^{-1}$ .

Figure 11 b) shows an amplification of the Raman spectrum where, interestingly, around  $1510\text{ cm}^{-1}$  HPMC-Olz film revealed a mild peak, comparing to the physical-mixture spectrum. Also referring to HPMC-Olz film, peaks between  $1510\text{-}1604\text{ cm}^{-1}$  in Figure 11, these were deviated towards higher wavenumbers, comparing to HPMC-Olz's physical-mixture curve.

Besides the fact that the region between  $1510\text{-}1600\text{ cm}^{-1}$  was defined as a good-differentiator between polymorphs of olanzapine, is it also the region where azepine's NH deformations (among other contributions) are assigned (22), which suggests that some interaction via NH groups could be happening.

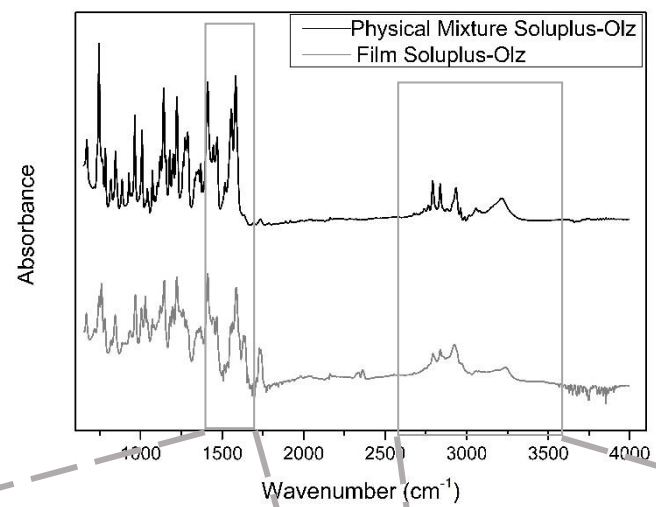
### Soluplus-Olanzapine

Figures 13 and 14 display the Raman and IR spectra obtained for Soluplus-Olanzapine physical mixture and films. It is interesting that both curves are more similar to one another, than the ones with HPMC-olanzapine products. An in-depth analysis is made in the following chapter (chapter 5).

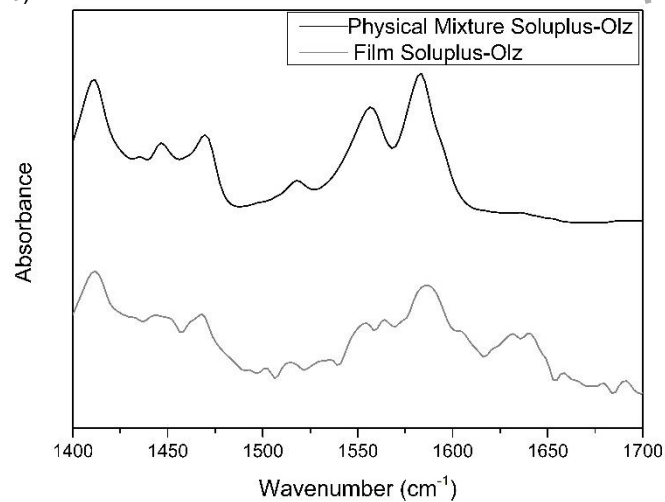


**Fig. 13** Raman spectrum of Soluplus-Olz physical mixture and film: a) background; b) Raman shift  $1400\text{-}1700\text{ cm}^{-1}$ .

a)



b)



c)

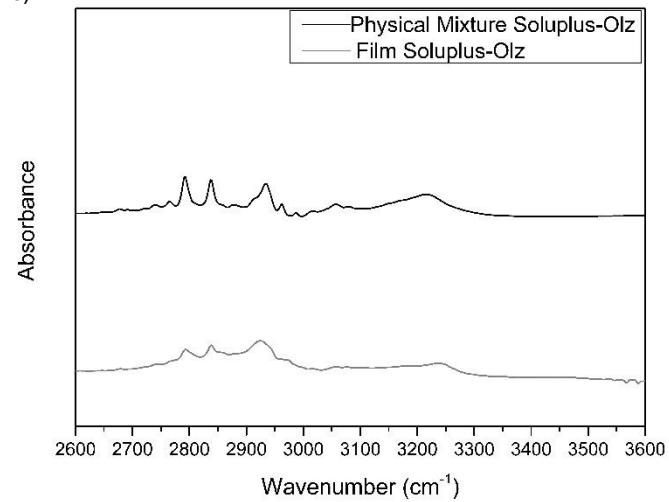
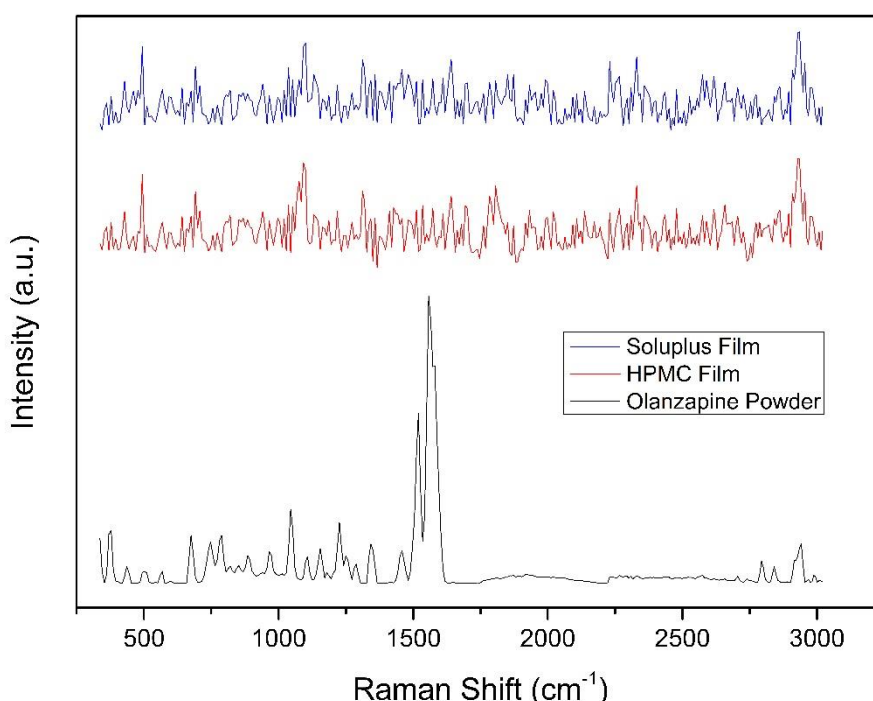


**Fig. 14** ATR IR spectrum of Soluplus-Olz physical mixture and film: a) full spectra; b) 1400-1700 cm<sup>-1</sup> and c) 2600-3600 cm<sup>-1</sup>.



Regarding Figure 13 b), a mild peak was found at wavenumber  $1509\text{ cm}^{-1}$  for the Soluplus-Olz film. The presence of this protuberance interferes with the typical well-defined curve of form 1 olanzapine, as only form 2 reveals a peak in this region (Table 3). These finding could indicate a presence of form 2, although no other relevant features of form 2 were seen in the spectrum. Once again, peaks were found shifted towards higher wavenumbers, which is usually a sign of interaction between compounds, or a sign of the presence of different polymorphs. Adding to the fact that these region of the spectrum was assigned to NH deformations, the intensity of the peak at  $1520\text{ cm}^{-1}$  could suggest that an interaction could be occurring between the drug and the polymer through this group (22).

With the aim of choosing an accurate wavenumber to focus in CARS, a Time Gated Raman was performed. Figure 15 shows the different obtained spectra. As there is no overlapping in the range of  $1500$  and  $1700\text{ cm}^{-1}$ , this was the wavenumbers chosen to use in CARS.



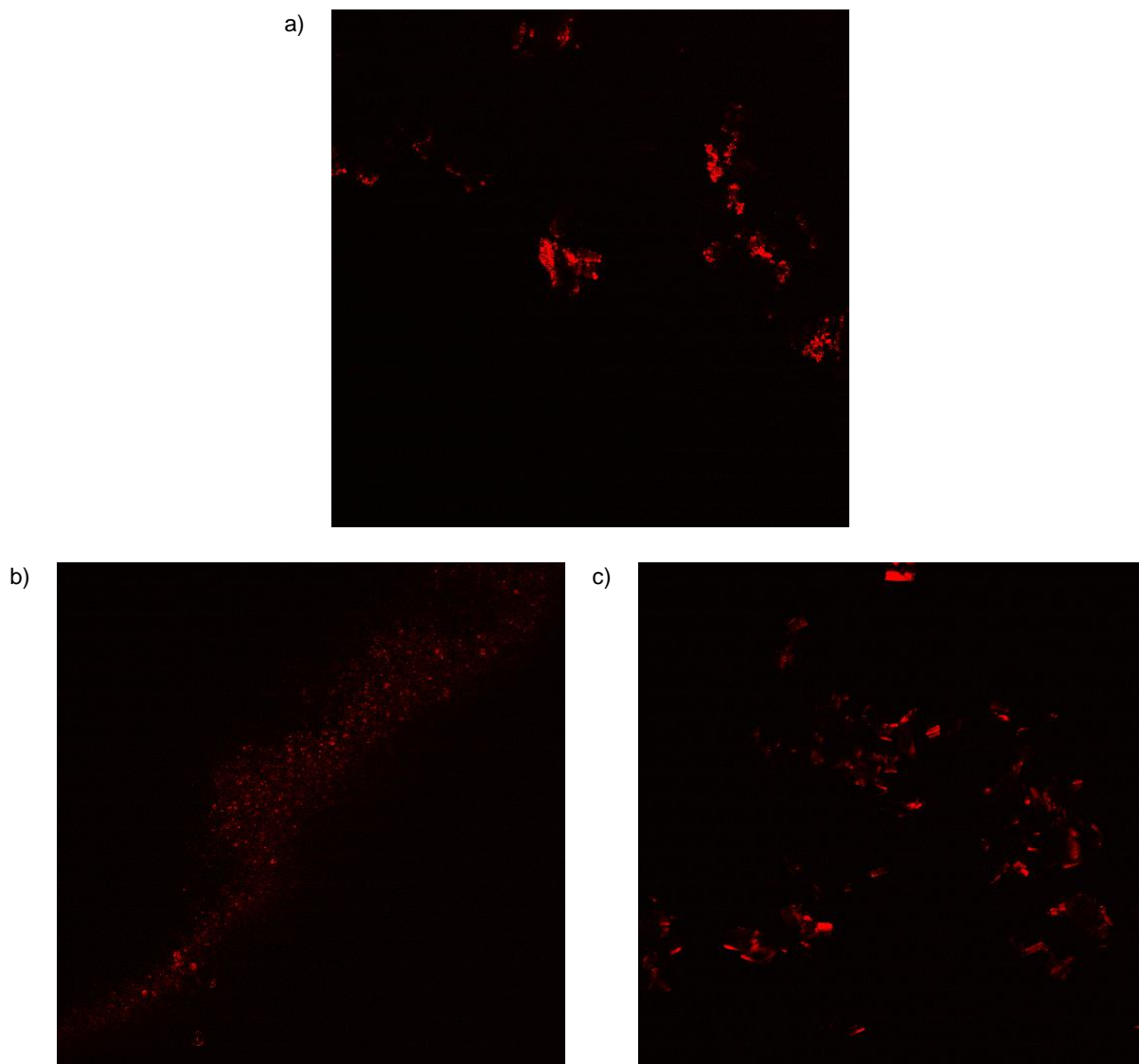
**Fig. 15** TGR spectrum of Olanzapine powder, Soluplus film and HPMC film in the range  $264$ - $3100\text{ cm}^{-1}$ . The intensity of Soluplus and HPMC spectra are not to scale with olanzapine powder.

Figure 16 a) shows the CARS imaging results for olanzapine powder. Despite the lack of signal when the second harmonic test was performed (due to the centrosymmetric dimers of this drug), the strong red signal in Figure 16 a) leads one to conclude that is possible to obtain a signal for olanzapine at the wavenumber used. It is relevant to mention that the second harmonic test is generally useful to test if a signal comes indeed from the presence of the drug.

Figures 16 b) and c) show the results for polymer-drug films. Both were captured with the same amplification, therefore, these images suggest that Soluplus-Olz film possesses crystals with bigger dimensions than HPMC-Olz ones.

Furthermore, these results inform about the spatial distribution of the active ingredient. It is noticeable that both samples revealed to be relatively inhomogeneous, as some areas of each film showed higher concentration of olanzapine than other parts. In this matter, HPMC suggests a higher dispersion, as the smaller crystals appear to be better distributed throughout

the image (Fig. 16 b)), while Soluplus-film revealed bigger crystals which means that homogeneity is harder to achieve.



**Fig. 16** CARS imaging of: a) olanzapine powder -  $\omega_n = 1517 \text{ cm}^{-1}$ ; b) HPMC-Olz film -  $\omega_n = 1517 \text{ cm}^{-1}$ ; c) Soluplus-Olz film -  $\omega_n = 1517 \text{ cm}^{-1}$ .

## 4.5 DSC characterization

### 4.5.1 Starting Materials

DSC results of the drug show a well-defined narrow endothermic peak with  $T_{\text{onset}}$  of 194.10°C (Fig. 17), which is in keeping with the literature (21, 23). The melting heat was found to be -115 J/g. Hence, one can conclude that olanzapine raw material was the polymorph form 1.

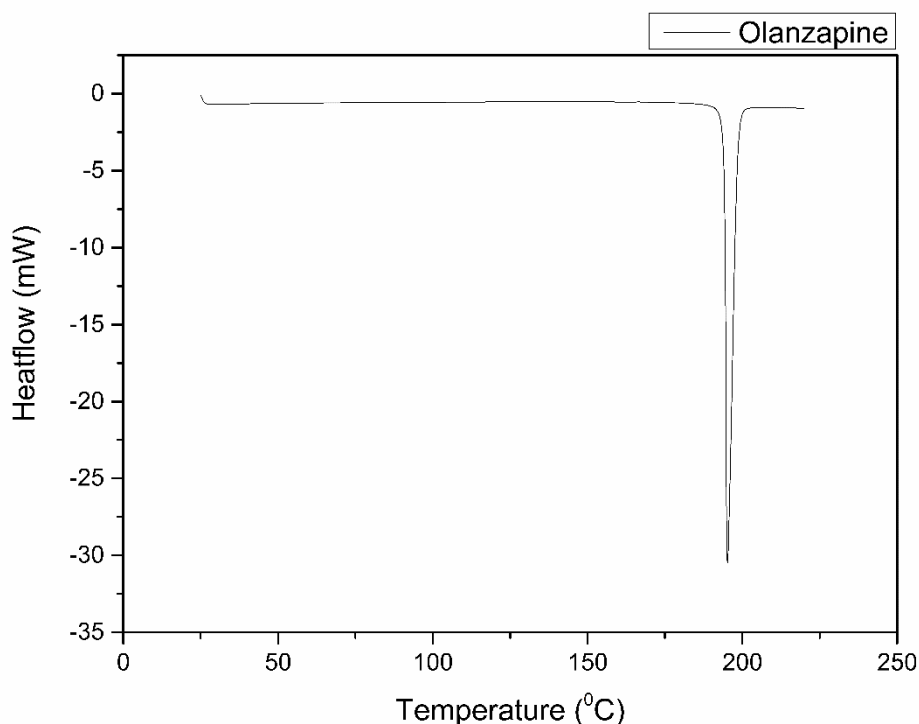


**Fig. 17** DSC curve of olanzapine powder.

Respective to Figure 18, the DSC curve of the HPMC raw material showed a broad endothermic inflection which corresponds to the dehydration of the polymer, and the temperature range of this event appeared to be between 30-110 °C (Figure 18). Preceding the only exothermal elevation of the curve, as well as after that event, there are mild endothermic depressions. This could be associated with the presence of semi-crystalline form of HPMC due to the aging of the raw material. The glass transition temperature (described to be around 170°-180 °C in the literature) can be hidden in one of these inflections, which could be elucidated using MDSC, however this was not done because it is not concerned in the scope of this present work, as it would be too much time consuming.

The DSC curve of Soluplus raw material (Fig. 18) reveals a broad dehydration endothermic event in a range of 30-110°C, which was expected since this is a hygroscopic polymer. This depression of the curve contains the glass transition temperature, that is described to be at 70°C, and it seems to correspond to the obtained in this case (19, 35). It is to be noticed that a possible relaxation of the polymer could be happening in this temperature range as well, which means that this event is also covered in the broad endotherm referred previously.

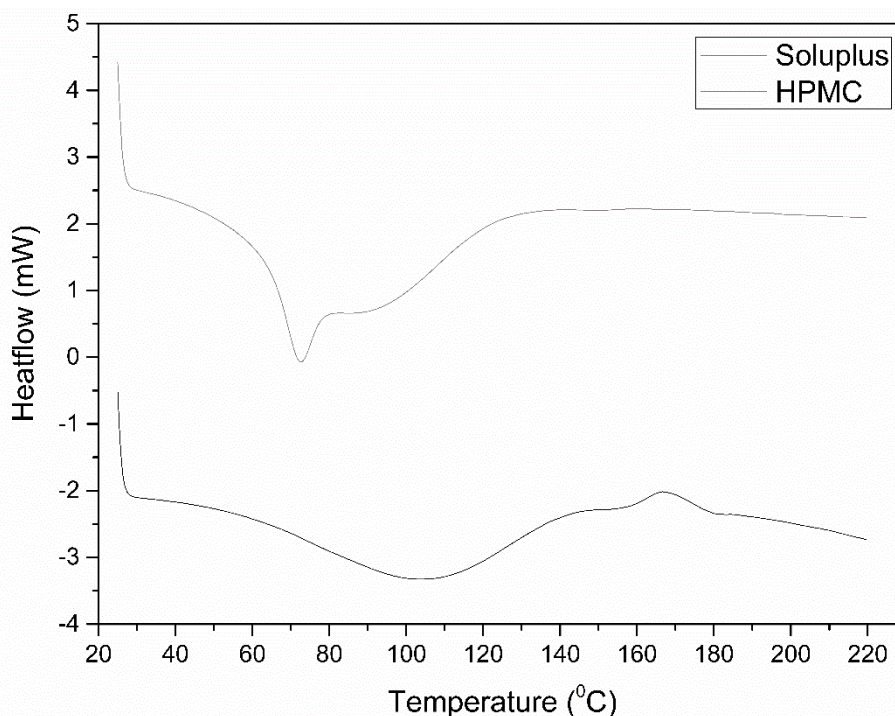


**Fig. 18** DSC curve of HPMC and Soluplus powder.

#### 4.5.2 Physical Mixtures and Films

Analysing the HPMC-olanzapine physical mixture first (Fig. 19), the inflection of the curve corresponding to the desolvation of the sample is followed with a well-defined endothermic peak. This has  $T_{\text{onset}}$  of 189.28 °C, which corresponds to the melting of olanzapine (5). It is important to highlight the shift in this temperature. This suggests that an interaction could be happening between the polymer and the drug.

Now focusing on the upper curve (HPMC-Olz film in Fig. 19), it shows a broad event of desolvation at first. It is also possible to see that the baseline of the curve before the endothermic event is lower than afterwards. This corresponds to the desolvation of methanol and possible some water content present in the film, which alters the heat capacity of the material. Of note is an exothermic event occurring with a  $T_{\text{onset}}$  of 112.63 °C. The hypothesis of a total conversion from amorphous to crystalline form can be ruled out because the heat energy is not the same as the next endothermic event of the curve ( $5,00 \text{ Jg}^{-1}$  for the exothermic event and  $-47.64 \text{ Jg}^{-1}$  for the endothermic one), i.e, some conversion could be happening, although there was some crystalline form present from the beginning as well.

The  $T_{\text{onset}}$  of the melting event is also shifted to lower temperature (179.85 °C). Once again, this supports the evidence of an interaction between both components.

The curve regarding the Soluplus-Olanzapine physical mixture (Fig. 19) possesses a broad depression where there is the  $T_g$  around 70 °C.

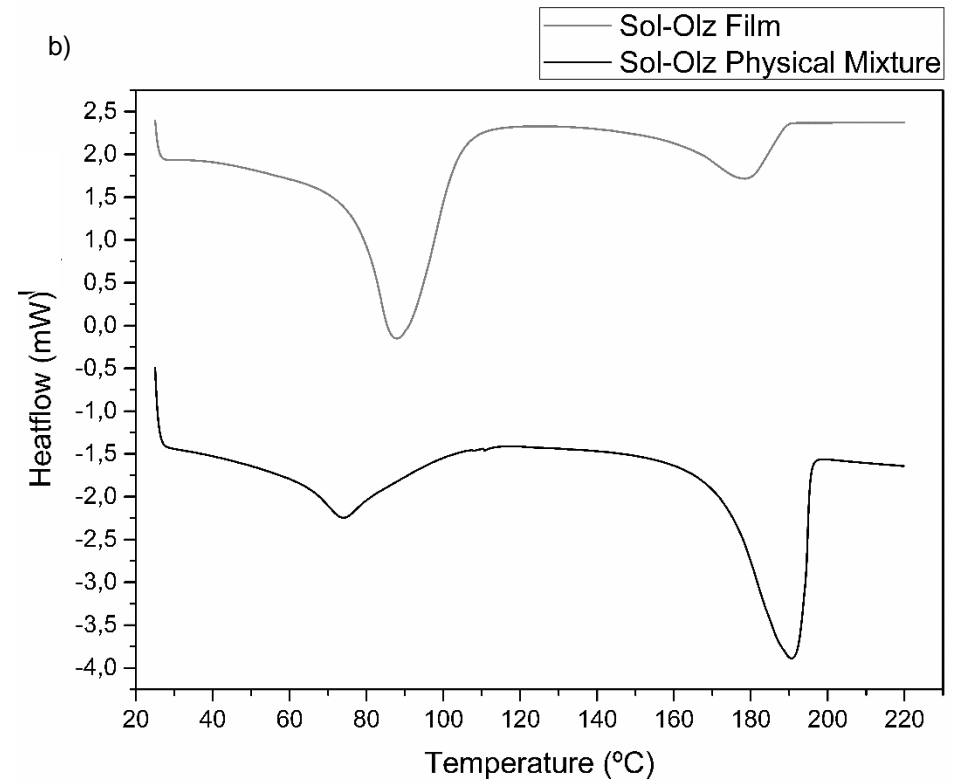
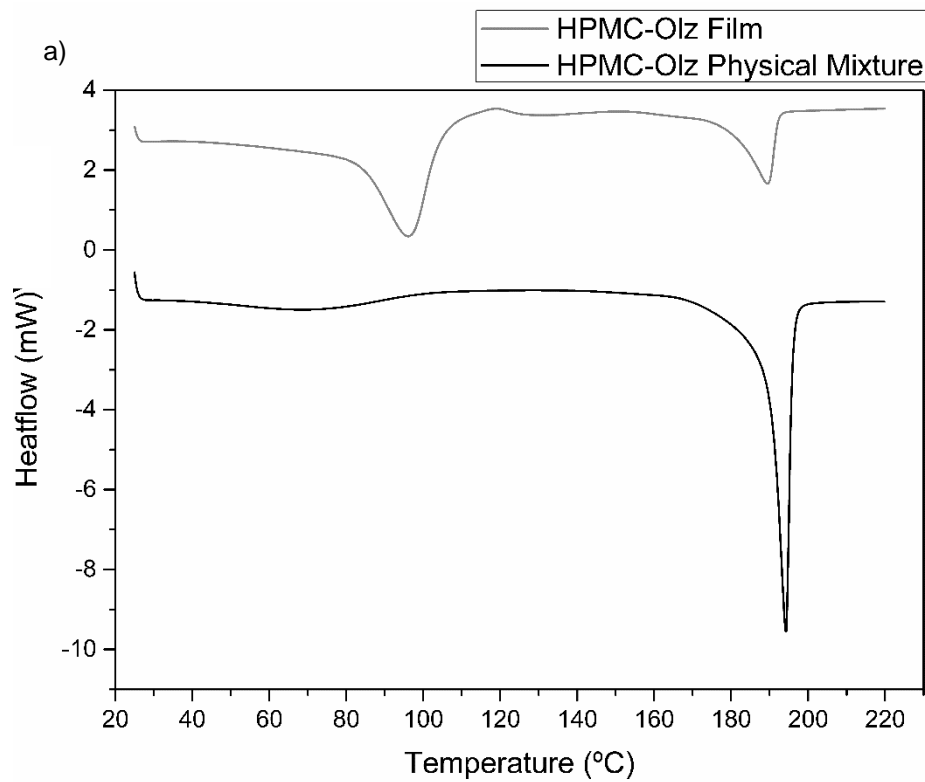


**Fig. 19** DSC curve of a) HPMC-Olz physical mixture (bottom curve) plotted against HPMC-Olz film (upper curve); b) Soluplus- Olz physical mixture (upper curve) plotted against Sol-Olz film (bottom curve).

The physical mixture Soluplus-olanzapine does not overlap at all with the curve obtained with form 1 olanzapine. Not only is there not a well-defined endothermic peak, but also the  $T_{\text{onset}}$  is severely dislocated to lower temperature.

Analysing the upper curve of Fig. 19, there is a desolvation event starting at lower temperature, which appears to be more prominent than the same event in the physical mixture (which is predictable). A broad endothermic has a  $T_{\text{onset}}$  of 157.48 °C.

**Table 4** Compilation of DSC data obtained from olanzapine raw material, HPMC-Olz and Soluplus-Olz both physical mixture and film.

Sample	$T_{\text{onset}}$ exothermal event (°C)	$\Delta H$ (Jg <sup>-1</sup> ) (exothermic)	$T_{\text{onset}}$ melting (°C)	$\Delta H$ (Jg <sup>-1</sup> ) (endothermic)
Olanzapine Raw Material	-	-	194.18	119.03
HPMC-Olz Physical Mixture	-	-	189.28	59.76
HPMC-Olz Film	112.63	5.00	179.85	47.64
Soluplus-Olz Physical Mixture	-	-	170.22	41.98
Soluplus-Olz Film	-	-	157.48	29.83

Table 4 resumes the DSC results obtained from all the samples.

## 5. Discussion

### 5.1 Starting Materials - Powders

Based on Table 3, one can verify the similarities between Raman and IR spectra of the starting material and the features of form 1 olanzapine described in previous works. As stated before, special attention should be placed in the region between 1400-1700  $\text{cm}^{-1}$  of Raman spectrum (Fig. 9 b)), where no splitting has occurred near 1518  $\text{cm}^{-1}$ . Additionally, most of the peaks found are much closer to the form 1 description rather than to form 2 (Table 3). Thus, the raw material of the drug is, most certainly, form 1 polymorph. Also, the DSC results of the drug show a well-defined narrow endothermic peak with  $T_{\text{onset}}$  of 194.10  $^{\circ}\text{C}$  which is in conformity with the literature (21, 23). The melting heat was found to be -115 J/g. According with both works of Polla *et al.* and Peres-Filho *et al.*, in case of form 1, this is the only phenomenon found in the thermal curve. The curve obtained in this present work shows the same behaviour, reinforcing the previous statement of the raw material is, in fact, form 1 olanzapine (21, 23).

### 5.2 Physical Mixtures and Final Products

Once defined the solid form of the starting materials, an attempt of characterizing the solid state of the drug in the final product, as well as possible interactions between the polymers and the drug, were made.

The polarized light microscopy showed some refringence, which revealed the presence of crystals in the final films (Fig. 8). This fact and the observation of opaque films came to confirm the statement of being in the presence of a two-phase system. Thus, the possibility of having an amorphous form and a molecular dispersion of the drug in the polymeric matrix was ruled out. The concentration of the casted solution should be one of the features to be studied and optimized in order to obtain a molecular dispersion.

With the aim of clarifying this question, an in-depth analysis of the spectroscopic data was performed.

Regarding the HPMC-Olanzapine physical mixture and film, one can find some characteristic peaks of olanzapine, although they are clearly not correspondent to crystalline form 1. Looking closer to the Raman spectra between wavenumbers 1590-1605  $\text{cm}^{-1}$  (Fig. 11 b)), besides the fact that the bands are deviated towards higher wavenumbers, there is a mild peak at 1510  $\text{cm}^{-1}$  (which would not be present at all in case of form 1). Despite this finding, most of the other peaks are somehow shifted from the typical spectra of form 2 as well, which means that it is not form 2 either. Because the producing conditions of the films used methanol as solvent and did not involve drying with heat, the possibility of having a methanolate should not be excluded.

The results in table 3 could suggest that there is an interaction occurring between HPMC and olanzapine. If this is the case, the interaction would be, most probably, taking place through H bonds between the nitrogen H donor and acceptors of the drug and the multiple oxygen H donors and acceptors of the polymer. This hypothesis is supported by the several shifts observed in the spectrum of HPMC-Olz films. For instance, in Figure 12 c), it is possible to see that the zone of the vibration modes of OH in the film's spectra has suffered a significant change comparing to the physical mixture. Another important observation is the deviation of NH stretching vibration of R2 ring, that is almost unnoticeable in the IR spectrum (Fig. 12 c)), but visible in Raman spectrum (Fig. 11 b).

Severe changes are also seen in Figure 12 spectrum, taking into account the HPMC powder's spectra (Fig. 10 a) and c) comparing to Fig. 12 a) and c)), where the characteristic

range of OH groups are clearly very different from the ones in the physical mixture and in the film ( $\omega_n$  3460  $\text{cm}^{-1}$ ). This also supports the involvement of these groups in the interaction between the two components.

In fact, previous studies showed that azepine's NH (R2) is capable of interacting with other molecules, due to the preserved dimeric cell unit that allows hydrogen bond donors and acceptors to remain available for hydrogen bonding (22, 25).

What was previously described for HPMC-Olz films also happens with Soluplus polymer. The Raman and IR spectrum of the film resemble the ones obtained from the physical mixture of the polymer and the drug. In these spectra, there are some olanzapine peaks that are recognizable, such as 1603, 1588, 1562  $\text{cm}^{-1}$  (Fig. 13), although they are shifted towards higher wavenumbers, as it happened with the HPMC-Olz film.

It is visible once again the mild peak at 1509  $\text{cm}^{-1}$  in Raman spectrum (Fig. 13 b)), excluding the possibility of olanzapine being present as form 1 polymorph. Table 3 also shows several deviations found between wavenumbers of form 1, form 2 and the obtained spectrum, both for Raman and IR spectrum.

Regarding IR spectrum of Soluplus-Olz film, the big features of the physical mixture's spectra seem more preserved. Nevertheless, Fig. 14 illustrates some noticeable deviations that might suggest some interaction between both components. The fact that the band correspondent to OH vibration modes is shifted to higher wavenumbers, gives a clue to the origin of the interactions. The interaction, to be happening, should be via H bonds between nitrogen acceptor atom of olanzapine and the oxygen donor of Soluplus.

Referring to both HPMC- and Soluplus-Olz films, none of the spectra reveal similarities with the IR spectra of the amorphous form given by the patents found in the literature (28), which reinforces the possibility of not being in the presence of amorphous form either, supporting what was hypothesized previously.

One feature that could contrapose and make this discussion more complex is the very high chance of being in the presence of a methanolate form of olanzapine in the films. In that case, H bonds would be involved through diazepine N10 donor and piperazine N4 acceptor (of a different molecule), acting the methanol as both H donor and acceptor (26). Thus, the shifts seen in the spectrum may come from the H bonding between olanzapine and the methanol, and could be mimicking an interaction between the drug and the polymer.

To the best of our knowledge, no previous reports of methanolate spectroscopic data that could help to elucidate this issue have been published.

Beginning with analysing the DSC curve of the physical mixture of HPMC with olanzapine (Fig. 19), an inflection of the curve corresponding to the desolvation of the polymer is visible, where its  $T_g$  is hidden, followed by a well-defined endothermic peak that is shifted relatively to olanzapine's melting event seen in case of the pure drug. This suggests that an interaction is happening between HPMC and Olanzapine.

Now focusing on the HPMC-Olz film's curve in Figure 19, there is an exothermic event occurring with a  $T_{\text{onset}}$  of 112.63  $^{\circ}\text{C}$ . The hypothesis of a total conversion from amorphous to crystalline form can be ruled out because the heat energy is not the same as the next endothermic event of the curve (5.00  $\text{Jg}^{-1}$  for the exothermic event and -47.64  $\text{Jg}^{-1}$  for the endothermic one), i.e, some conversion could be happening, although there was some crystalline form present from the beginning as well. The desolvation of solvent molecules present in the sample would also occur in the range between 110-120  $^{\circ}\text{C}$ , according with other results found in the literature.

The  $T_{\text{onset}}$  of the melting event is also shifted to lower temperature (179.85  $^{\circ}\text{C}$ ). Once again, this supports the evidence of an interaction between HPMC and olanzapine.



Regarding Soluplus-Olanzapine physical mixture (in Fig. 19), it possesses a broad depression where there is the  $T_g$  around 70 °C. The physical mixture of soluplus and olanzapine does not overlap at all with the curve obtained with form 1 olanzapine. Not only there is not a well-defined endothermic peak, but also the  $T_{onset}$  is severely dislocated to lower temperature. This finding reveals a strong interaction upon heating between the polymer and the drug, even at a physical mixture level.

Analysing the Sol-Olz film's curve if Figure 19, there is a desolvation event starting at lower temperature, which appears to be more prominent than the same event in the physical mixture (which is predictable). As opposed to HPMC case, no crystal conversion is visible with Soluplus, as no exothermic event is shown. However, a broad endothermic event occurring with a  $T_{onset}$  of 157.48 °C is also visible. Thus, there seems to exist an interaction between the drug and this polymer. This melting event suggests that some crystals were already present in the film, which proposes that it does not correspond to a molecular dispersion.

It is important to notice that DSC results are induced by the high temperatures of the method itself, thus, they may not reflect the transformations that the product undergoes during its shelf-life (at 25°C).

CARS imaging revealed that Soluplus-olanzapine films had crystals with bigger dimensions than HPMC-Olanzapine films. This seems to be congruent with what has been found in the DSC results, as the last film could contain some amorphous olanzapine.

From this analysis, one can verify that the film does not represent a molecular dispersion, since there were some crystals present previously to the measurements. Nevertheless, these DSC results strongly suggest that some interaction could be occurring between the polymer and the drug. Based on the displacement extension, this interaction appears to be stronger in the case of Soluplus, comparing to HPMC, since the melting events are more shifted in the former case. It is important to keep in mind that soluplus has a more amphiphilic character when compared to HPMC, which is more hydrophilic. This means that soluplus would be capable of interact in a greater extent via weaker interactions than HPMC. Consequently, the probable interactions between the polymers and the drug are H bonding.

As stated previously, an interaction does not mean incompatibility and, hence, these interactions could be of interest with the purpose of stabilizing amorphous-olanzapine or small dimensions of crystalline-olanzapine solid dispersions. Although the nature of these interactions is not well-defined with this project, it was found that both polymers seem suitable for further steps in development of olanzapine orodispersible films.

## 6. Conclusion

For the development of an orodispersible film through solvent-casting technique, a polymer capable of conferring viscosity to the solution to be casted is of utmost interest, especially when a casting device is used. In this way, HPMC had the advantage over Soluplus of facilitating the step of casting the solution on a Teflon plaque. HPMC- and Soluplus-Olz films in the proportion of 1:1 (m/m %) were very brittle and fragile, which is proposed to be improved using lower proportion of olanzapine, as well as using a Petri dish to cast the solution. The former solution would enhance the cross-link between side chains of the polymer, and the last one would allow the film to be thicker, hence, improving the mechanical properties of the obtained film.

A two-phase system was obtained, and crystals of olanzapine were found in both cases of olz-polymer films. Comparing to the assignment made in previous works and to the spectra obtained in this work, spectroscopic data showed peaks that did not correlate neither to form 1 nor to form 2. Furthermore, peaks were found to be shifted towards higher wavenumbers, namely peaks assigned to olanzapine's NH deformations. Additionally, alterations in the regions corresponding to polymer's OH groups were found, indicating that the interaction with the drug could happen through H bonding.

DSC results showed a melting point with a  $T_{\text{onset}}$  dislocated from the one described for olanzapine form 1 (in both cases of physical-mixtures and obtained films). Interestingly, the lower melting point seen for the case of physical-mixtures were aggravated in the case of the obtained films, being Soluplus the polymer with more severe deviations. Although thermal events in a DSC analysis are impelled by the elevated temperatures, the results support the possibility of occurring an interaction between drug and the polymers. To be noticed that, even though HPMC offers more sites of interactions, Soluplus appears to interact in a greater extent with olanzapine. This could be explained with its higher amphiphilic character, which may establish hydrophobic interactions with the drug.

The results of the present work point to what appears to be an interaction between olanzapine and polymers, through H bonding. Nonetheless, this interaction could be favourable as it could be interesting to stabilize small dimension crystals or even amorphous form of olanzapine.

## 7. Further Studies

To find more in-depth answers to this subject, further studies involving production and characterization of amorphous and methanolate forms would be necessary. Next steps would go through the study of different proportions between polymer and the drug. Due to the presence of substances with high glass transition temperature, it would be interesting to develop a solid dispersion where olanzapine would be in the amorphous state.

It would be of great interest to proceed to stability tests, as it is well known that the olanzapine methanolate is not stable for prolonged periods of time. In fact, Cavallari *et al.* found that after two weeks, the endothermic events of desolvation are no longer present in the DSC profiles (5).

Additionally, another variable relevant to study would be the change of casted-solution's concentration, as well as the comparison with other production techniques, once the solid state highly depends on the method used.

## 8. References

1. Hoffmann EM, Breitenbach A, Breitzkreutz J. Advances in orodispersible films for drug delivery. *Expert Opinion on Drug Delivery*. 2011;8(3):299-316.
2. Florence AT, Attwood D. *Physicochemical Principles of Pharmacy*. 4<sup>th</sup> ed: Pharmaceutical Press; 2006; 8-21.
3. Florence AT, Siepmann J. *Modern Pharmaceutics Volume 1: Basic Principles and Systems*. 5<sup>th</sup> ed: CRC Press; 2009; 253-303.
4. Bhardwaj RM, Price LS, Price SL, Reutzel-Edens SM, Miller GJ, Oswald IDH, et al. Exploring the Experimental and Computed Crystal Energy Landscape of Olanzapine. *Crystal Growth & Design*. 2013;13(4):1602-17.
5. Cavallari C, Santos BP-A, Fini A. Olanzapine Solvates. *Journal of Pharmaceutical Sciences*. 2013;102(11):4046-56.
6. Aulton ME. *Pharmaceutics: The Science of Dosage Form Design*. 2<sup>th</sup> ed: Churchill Livingstone; 2002; 141-148.
7. Teja SB, Patil SP, Shete G, Patel S, Bansal AK. Drug-excipient behavior in polymeric amorphous solid dispersions *Journal of Excipients and Food Chemicals*. 2013;4(3):70-94.
8. Atkins P, Paula Jd. *Physical Chemistry*. 9<sup>th</sup> ed: W. H. Freeman and Company; 2010; 697-709.
9. Levine IN. *Physical Chemistry*. 6<sup>th</sup> ed: McGraw-Hill; 2009; 913-946.
10. Siesler HW, Ozaki Y, Heise HM. *Near-Infrared Spectroscopy*. 1<sup>st</sup> ed: WILEY-VCH; 2002; 1-15.
11. TimeGate<sup>®</sup> Instruments. Raman and photoluminescence 2015 [Available from: <http://www.timegate.fi/timegated-raman/raman-and-photoluminescence/>; consulted on 22<sup>nd</sup> April 2017.
12. El-Diasty F. Coherent anti-Stokes Raman Scattering: Spectroscopy and microscopy. *Vibrational Spectroscopy*. 2010;55(1):1-37.
13. Tolles WM, Nibler JW, McDonald JR, Harvey AB. A Review of the Theory and Application of Coherent Anti-Stokes Raman Spectroscopy (CARS). *Applied Spectroscopy*. 1977;31(4):253-71.
14. Efremov EV, Ariese F, Gooijer C. Achievements in Resonance Raman Spectroscopy: Review of a technique with a distinct analytical chemistry potential. *Analytica chimica acta*. 2008;606(2):119-34.
15. Smith E, Dent G. *Modern Raman Spectroscopy - A Practical Approach*: John Wiley & Sons, Ltd; 2005; 93-112.
16. Weaver R. Rediscovering Polarized Light Microscopy. *American Laboratory*. 2003;35(20):55-61.
17. Clas S-D, Dalton CR, Hancock BC. Differential Scanning Calorimetry: Applications in drug development. *Pharmaceutical Science & Technology Today*. 1999;2(8):311-20.
18. Coleman NJ, Craig DQM. Modulated Temperature Differential Scanning Calorimetry: A Novel Approach to Pharmaceutical Thermal Analysis. *International Journal of Pharmaceutics*. 1996;135(1-2):13-29.
19. Nagy ZK, Balogh A, Vajna B, Farkas A, Patyi G, Kramarics Á, et al. Comparison of Electrospun and Extruded Soluplus<sup>®</sup> - Based Solid Dosage Forms of Improved Dissolution. *Journal of Pharmaceutical Sciences*. 2012;101(1):322-32.

20. Fussell AL, Grasmeijer F, Frijlink H, Boer AHd, Offerhaus HL. CARS microscopy as a tool for studying the distribution of micronised drugs in adhesive mixtures for inhalation. *Journal of Raman Spectroscopy*. 2014;45(7):495-500.
21. Peres-Filho MJ, Gaeti MPN, Oliveira SRd, Marreto RN, Lima EM. Thermoanalytical investigation of olanzapine compatibility with excipients used in solid oral dosage forms. *Journal of Thermal Analysis and Calorimetry*. 2010;104(1):255-60.
22. Ayala AP, Siesler HW, Boese R, Hoffmann GG, Polla GI, Vega DR. Solid state characterization of olanzapine polymorphs using vibrational spectroscopy. *International Journal of Pharmaceutics*. 2006;326(1):69-79.
23. Polla GI, Vega DR, Lanza H, Tombari DG, Baggio R, Ayala AP, et al. Thermal behaviour and stability in Olanzapine. *International Journal of Pharmaceutics*. 2005;301(1):33-40.
24. Bunnell CA, Hendriksen BA, Larsen SD, inventors; Eli Lilly and Company, assignee. Olanzapine Polymorph Crystal Form. USA patent 5,736,541. 1998.
25. Reutzel-Edens SM, Bush JK, Magee PA, Stephenson GA, Byrn SR. Anhydrates and Hydrates of Olanzapine: Crystallization, Solid-State Characterization, and Structural Relationships. *Crystal Growth & Design*. 2003;3(6):897-907.
26. Wawrzycka-Gorczyca I, Mazur L, Koziol AE. 2-Methyl-4-(4-methyl-1-piperazinyl)-10*H*-thienol[2,3-*b*][1,5]benzodiazepine methanol solvate. *Acta Crystallographica Section E: Structure Reports Online*. 2004;60(1):o69-o71.
27. Bunnell CA, Hotten TM, Larsen SD, Tupper E, inventors; Eli Lilly and Company, assignee. Process and Solvate os 2-Methyl-Thieno-Benzodiazepine. USA patent 5,703,232. 1997.
28. Gray J, inventor Amorphous Form of Olanzapine. USA patent 10/561,009. 2004.
29. Rowe RC, Sheskey PJ, Quinn ME. *Handbook of Pharmaceutical Excipients*. 6<sup>th</sup> ed: Pharmaceutical Press; 2009; 326-329.
30. Nagar P, Chauhan I, Yasir M. Insights into Polymers: Film Former in Mouth Dissolving Films. *Drug Invention Today*. 2011;3(12):280-9.
31. Yasmeen BR, Firoz S, Mouli YC, Vikram A, Mahitha B, Aruna U. Preparation and Evaluation of Oral Fast Dissolving Films of Citalopram Hydrobromide. *International Journal of Biopharmaceutics*. 2012;3(2):103-6.
32. Repka MA, Gutta K, Prodduturi S, Munjal M, Stodghill SP. Characterization of cellulosic hot-melt extruded films containing lidocaine. *European Journal of Pharmaceutics and Biopharmaceutics*. 2004;59(1):189-96.
33. Maher EM, Ali AMA, Salem HF, Abdelrahman AA. In vitro/In vivo Evaluation of an optimized fast dissolving oral film containing olanzapine co-amorphous dispersion with selected carboxylic acids. *Drug Delivery*. 2016;23(8):3088-100.
34. Zheng X, Yang R, Tang X, Zheng L. Part I: Characterization of Solid Dispersions of Nimodipine Prepared by Hot-melt Extrusion. *Drug Development and Industrial Pharmacy*. 2007;33(7):791-802.
35. Paaver U, Tamm I, Laidmäe I, Lust A, Kirsimäe K, Veski P, et al. Soluplus Graft Copolymer: Potential Novel Carrier Polymer in Electrospinning of Nanofibrous Drug Delivery. *BioMed Research International*. 2014:1-7.
36. BASF. Soluplus®. *Pharma Ingredients & Services*; 2010. p. 1-8.
37. Lan Y, Ali S, Langley N. Characterization of Soluplus by FTIR and Raman Spectroscopy. CRS 2010 Annual Conference, At Portland, Oregon, USA; 2010.

38. Pina MF, Zhao M, Pinto JF, Sousa JJ, Craig DQM. The Influence of Drug Physical State on the Dissolution Enhancement of Solid Dispersions Prepared Via Hot-Melt Extrusion: A Case Study Using Olanzapine. *Journal of Pharmaceutical Sciences*. 2014;103(4):1214-23.
39. Krishnamoorthy V, Nagalingam A, Prasad VPR, Parameshwaran S, George N, Kaliyan P. Characterization of Olanzapine-Solid Dispersions. *Iranian Journal of Pharmaceutical Research*. 2011;10(1):13-23.